



Material Discovery and High Throughput Exploration of Ru based Catalysts for Low Temperature Ammonia Decomposition

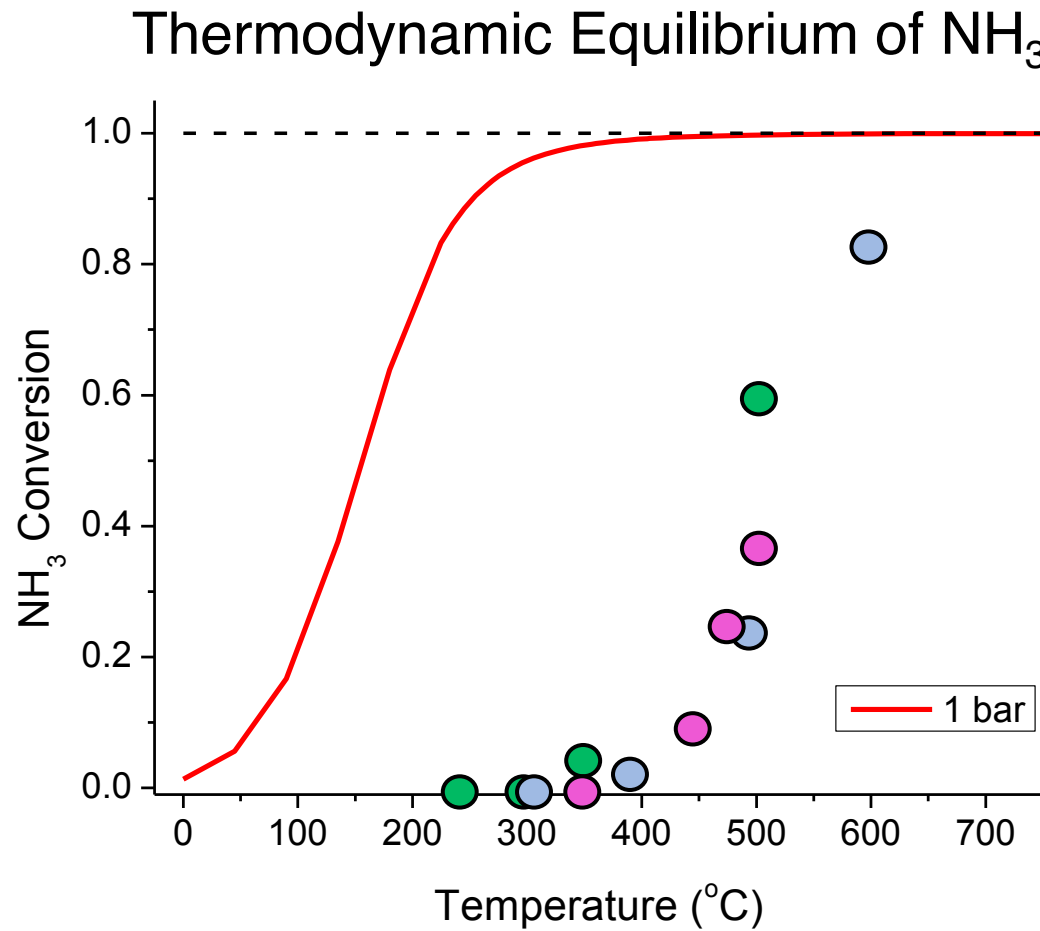
Katie McCullough, Travis Williams, Calvin Thomas and Jochen Lauterbach

October 31st 2018

Ammonia Fuel and Energy Storage: Cracking & Fuel Cells
AIChE Annual Conference

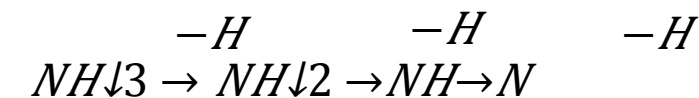
Pittsburgh, Transylvania

Thermocatalytic Ammonia Decomposition

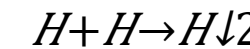
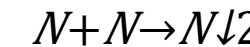


- Ru
- Ni
- Co

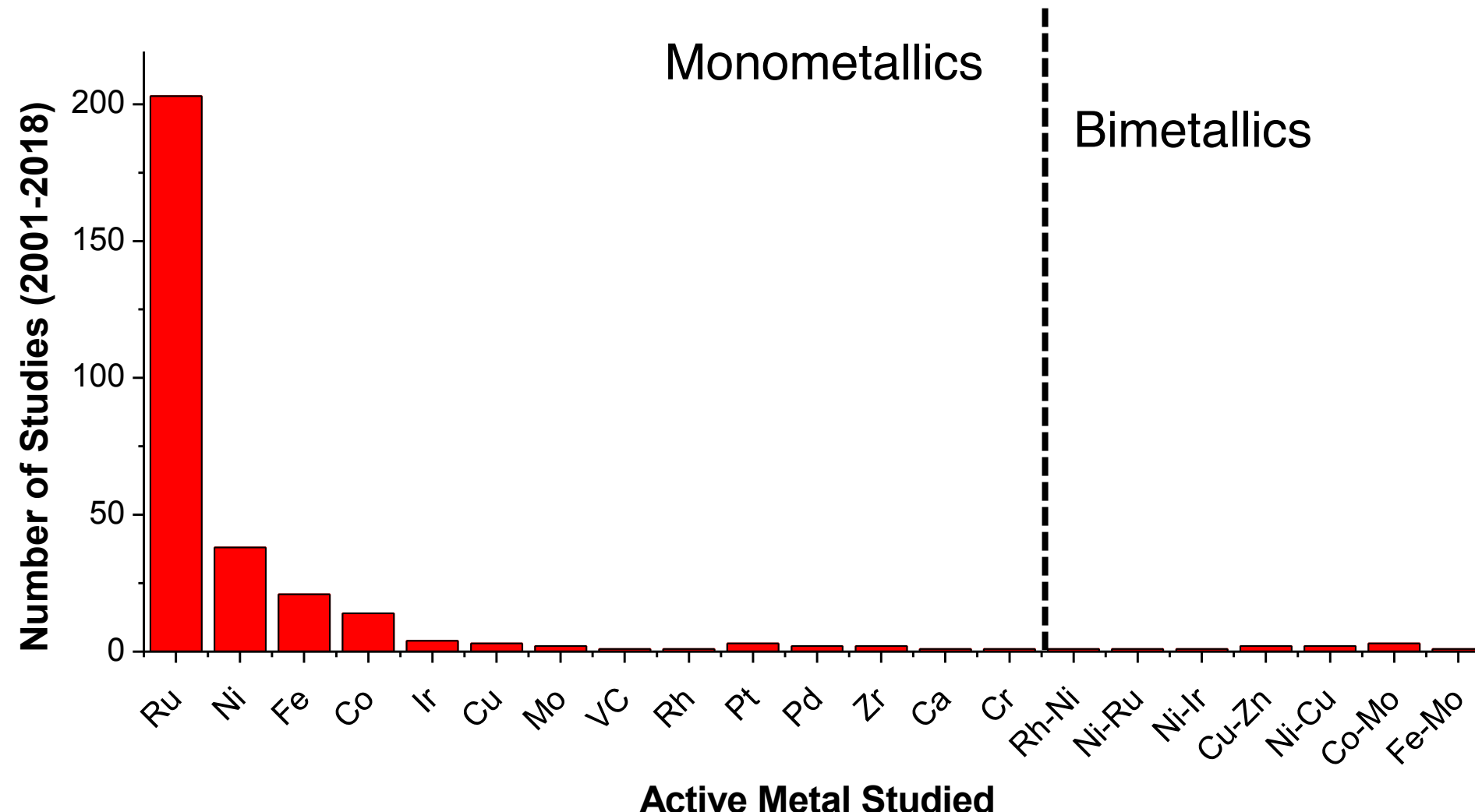
Dehydrogenation



Recombination



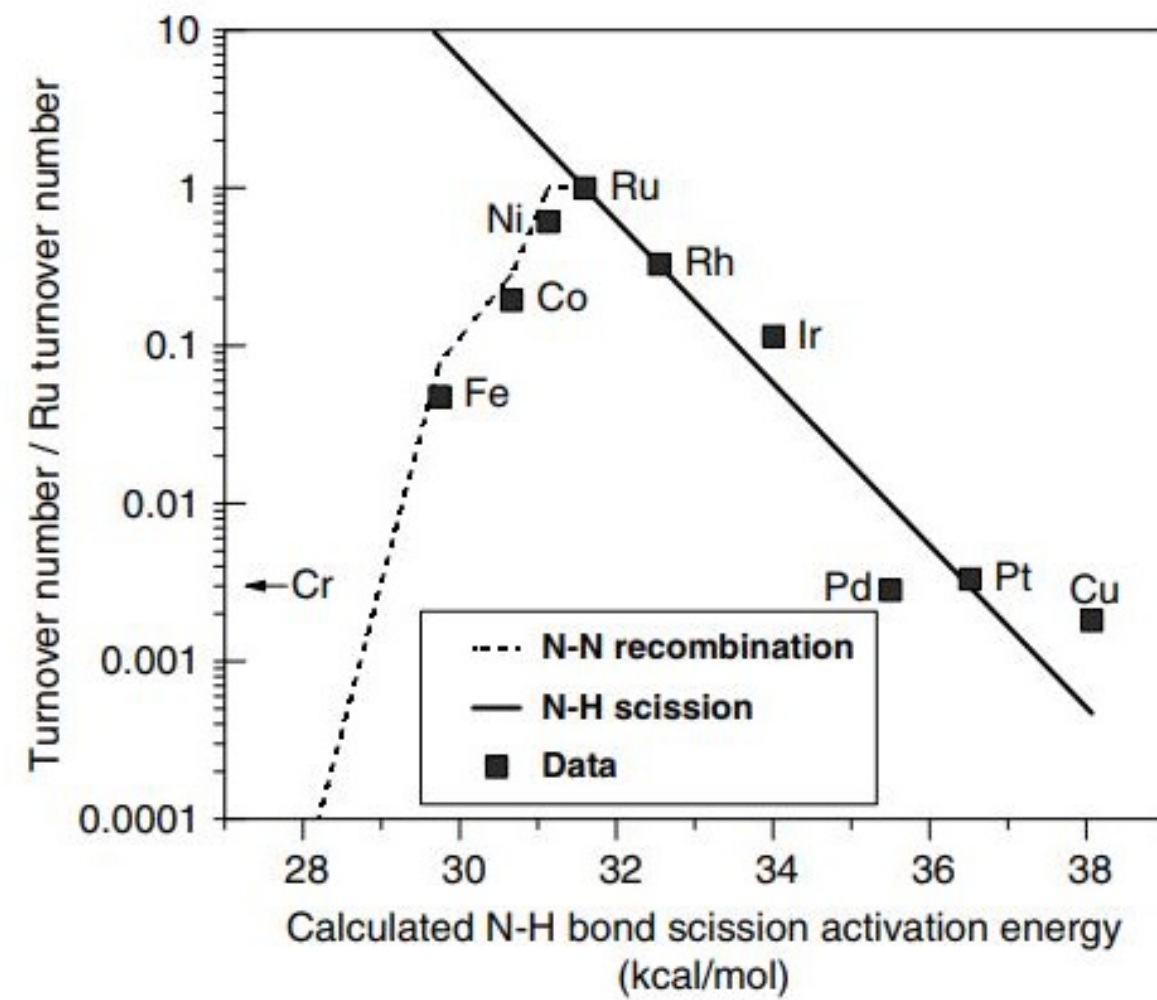
Materials for Ammonia Decomposition



Ammonia Decomposition

Many theoretical models exist that correlate different energies to NH_3 decomposition activity

No correlation found between 7 models and 13 metals



Design Space

PERIOD	GROUP	1	2	3	4	5	6	7	8	9	10	11	12	13	14	15	16	17	18
1	IA	1 1.008 H HYDROGEN	2 IIA Be BERYLLIUM																VIIA He HELIUM
2	IA	3 6.94 Li LITHIUM	4 9.0122 Be BERYLLIUM																2 4.0026 He NEON
3	IA	11 22.990 Na SODIUM	12 24.305 Mg MAGNESIUM	3 IIIB Sc SCANDIUM	4 IVB Ti TITANIUM	5 VB V VANADIUM	6 VIB Cr CHROMIUM	7 VIIB Mn MANGANESE	8 VIIIB Fe IRON	9 VIIIB Co COBALT	10 VIIIB Ni NICKEL	11 IB Cu COPPER	12 IB Zn ZINC	13 IIIA B BORON	14 IVA C CARBON	15 VA N NITROGEN	16 VIA O OXYGEN	17 VIIA F FLUORINE	18 VIIA Ne NEON
4	IA	19 39.098 K POTASSIUM	20 40.078 Ca CALCIUM	21 44.956 Sc SCANDIUM	22 47.867 Ti TITANIUM	23 50.942 V VANADIUM	24 51.996 Cr CHROMIUM	25 54.938 Mn MANGANESE	26 55.845 Fe IRON	27 58.933 Co COBALT	28 58.693 Ni NICKEL	29 63.546 Cu COPPER	30 65.38 Zn ZINC	31 69.723 Ga GALLIUM	32 72.64 Ge GERMANIUM	33 74.922 As ARSENIC	34 78.971 Se SELENIUM	35 79.904 Br BROMINE	36 83.798 Kr KRYPTON
5	IA	37 85.468 Rb RUBIDIUM	38 87.62 Sr STRONTIUM	39 88.906 Y YTTRIUM	40 91.224 Zr ZIRCONIUM	41 92.906 Nb NIOBIUM	42 95.95 Mo MOLYBDENUM	43 (98) Tc TECHNETIUM	44 101.07 Ru RUTHENIUM	45 102.91 Rh RHIDIUM	46 106.42 Pd PALLADIUM	47 107.87 Ag SILVER	48 112.41 Cd CADMIUM	49 114.82 In INDIUM	50 118.71 Sn TIN	51 121.76 Sb ANTIMONY	52 127.60 Te TELLURIUM	53 126.90 I IODINE	54 131.29 Xe XENON
6	IA	55 132.91 Cs CAESIUM	56 137.33 Ba BARIUM	57-71 La-Lu Lanthanide	72 178.49 Hf HAFNIUM	73 180.95 Ta TANTALUM	74 183.84 W TUNGSTEN	75 186.21 Re RHENIUM	76 190.23 Os OSMIUM	77 192.22 Ir IRIDIUM	78 195.08 Pt PLATINUM	79 196.97 Au GOLD	80 200.59 Hg MERCURY	81 204.38 Tl THALLIUM	82 207.2 Pb LEAD	83 208.98 Bi BISMUTH	84 (209) Po POLONIUM	85 (210) At ASTATINE	86 (222) Rn RADON
7	IA	87 (223) Fr FRANCIUM	88 (226) Ra RADIUM	89-103 Ac-Lr Actinide	104 (267) Rf RUTHERFORDIUM	105 (268) Db DUBNIUM	106 (271) Sg SEABORGIUM	107 (272) Bh BOHRIUM	108 (277) Hs HASSIUM	109 (276) Mt MEITNERIUM	110 (281) Ds DARMSTADTIUM	111 (280) Rg ROENTGENIUM	112 (285) Cn COPERNICIUM	113 (285) Nh NIHONIUM	114 (287) Fl FLEROVIIUM	115 (289) Mc MOSCOVIIUM	116 (291) Lv LIVERMORIUM	117 (294) Ts TENNESSEE	118 (294) Og OGANESSON
	LANTHANIDE	57 138.91 La LANTHANUM	58 140.12 Ce CERIUM	59 140.91 Pr PRASEODYMIUM	60 144.24 Nd NEODYMIUM	61 (145) Pm PROMETHIUM	62 150.36 Sm SAMARIUM	63 151.96 Eu EUROPIUM	64 157.25 Gd GADOLINIUM	65 158.93 Tb TERBIUM	66 162.50 Dy DYSPROSIUM	67 164.93 Ho HOLMIUM	68 167.26 Er ERBIUM	69 168.93 Tm THULIUM	70 173.05 Yb YTTERBIUM	71 174.97 Lu LUTETIUM			
	ACTINIDE	89 (227) Ac ACTINIUM	90 232.04 Th THORIUM	91 231.04 Pa PROTACTINIUM	92 238.03 U URANIUM	93 (237) Np NEPTUNIUM	94 (244) Pu PLUTONIUM	95 (243) Am AMERICIUM	96 (247) Cm CURIUM	97 (247) Bk BERKELIUM	98 (251) Cf CALIFORNIUM	99 (252) Es EINSTEINIUM	100 (257) Fm FERMIUM	101 (258) Md MENDELEVIUM	102 (259) No NOBELIUM	103 (262) Lr LAWRENCEIUM			

Copyright © 2017 Eni Generali

Incipient Wetness Impregnation

Baseline 4wt% Ru on Al_2O_3

Total 4wt% metal

3wt% Ru + 1wt% M

2wt% Ru + 2wt% M

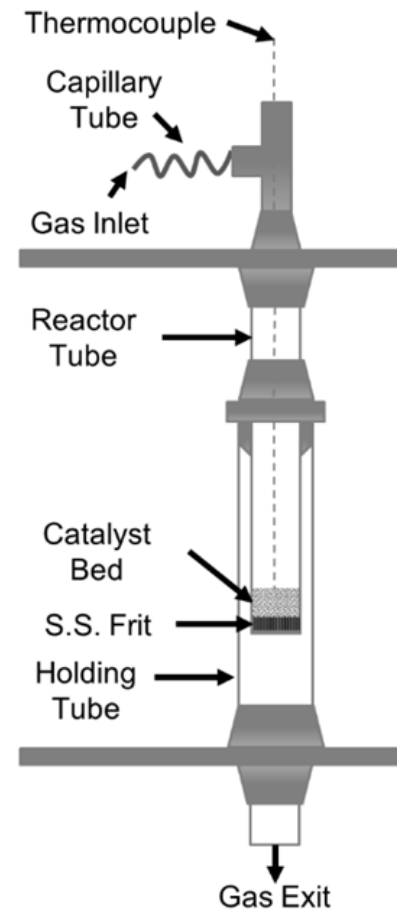
1wt% Ru + 3wt% M

+12 wt% K

105 unique formulations + repeats

High-Throughput Reactor System

- 16 parallel plug flow reactors
- Capillary flow distribution system
- Individual catalyst bed thermocouples
- Four furnaces with PID control (Tmax=950°C)
- Powder catalysts: 0.05-1 g
- Atmospheric pressure
- Moving top plate and winch system for efficient loading/unloading

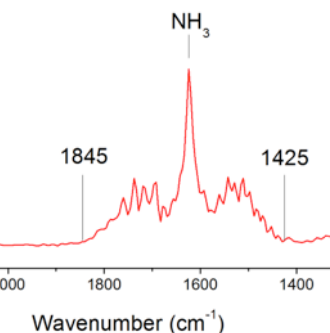
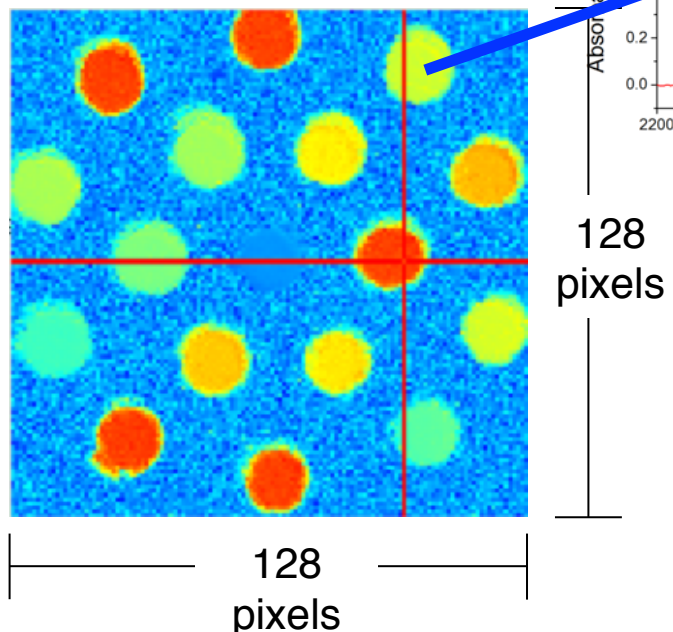


Effluent Gas Analysis

- IR gas-phase spectroscopy**

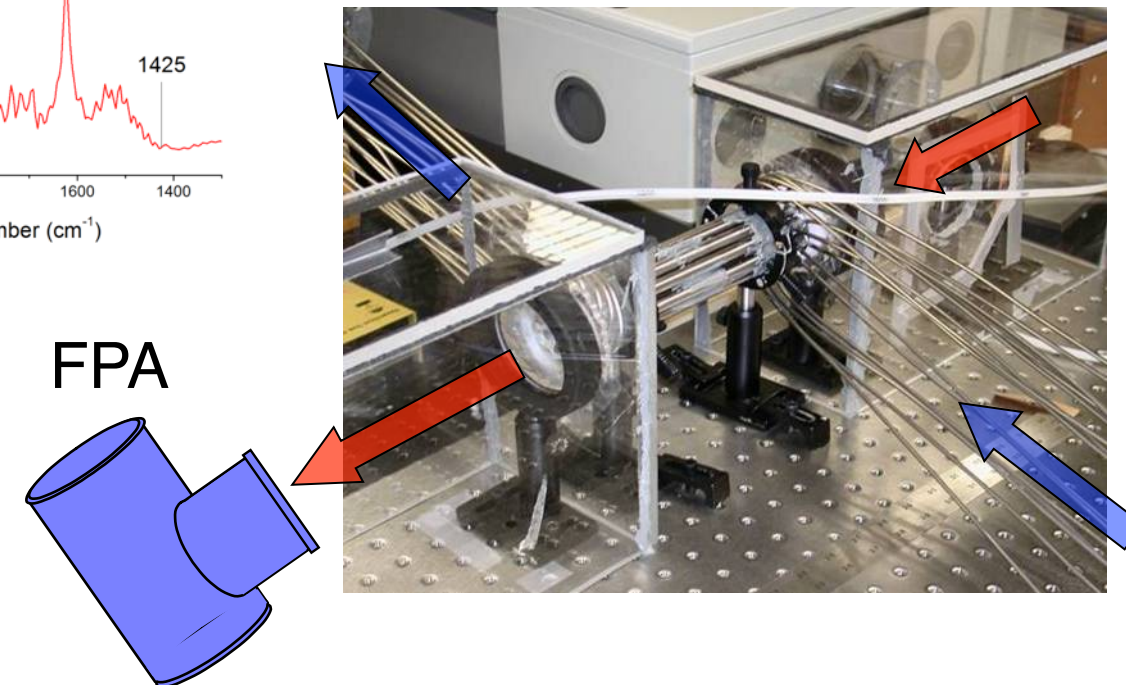
Works for any gas with IR signature

Spatially resolved IR spectra
 $128 \times 128 = 16,384$ detectors

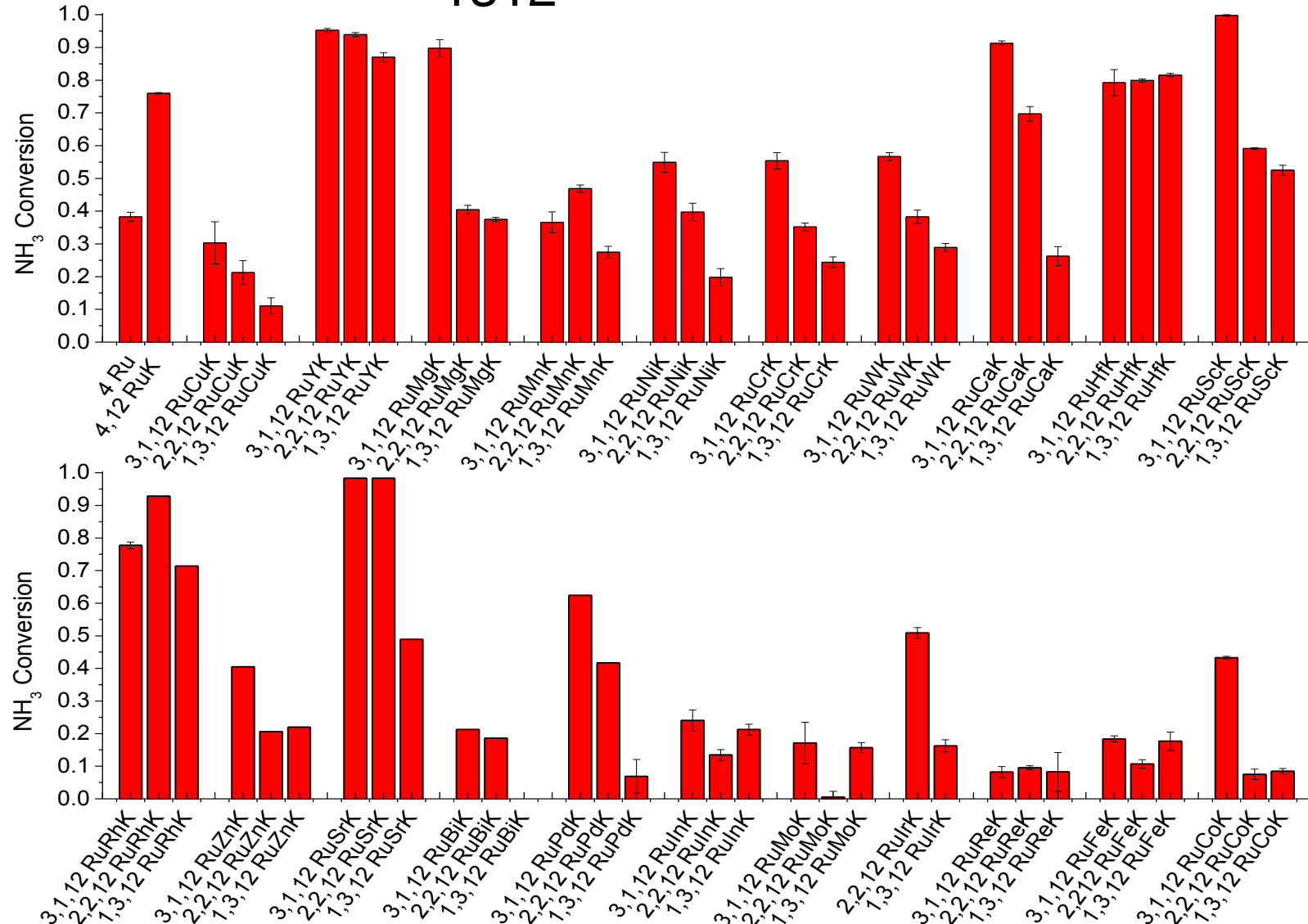


- 16-element gas-phase array**

Analyze all 16 product streams in parallel in < 2 sec



3112 Groupings of 2212 RuMK 1312



Reaction Conditions

Temperature = 300°C

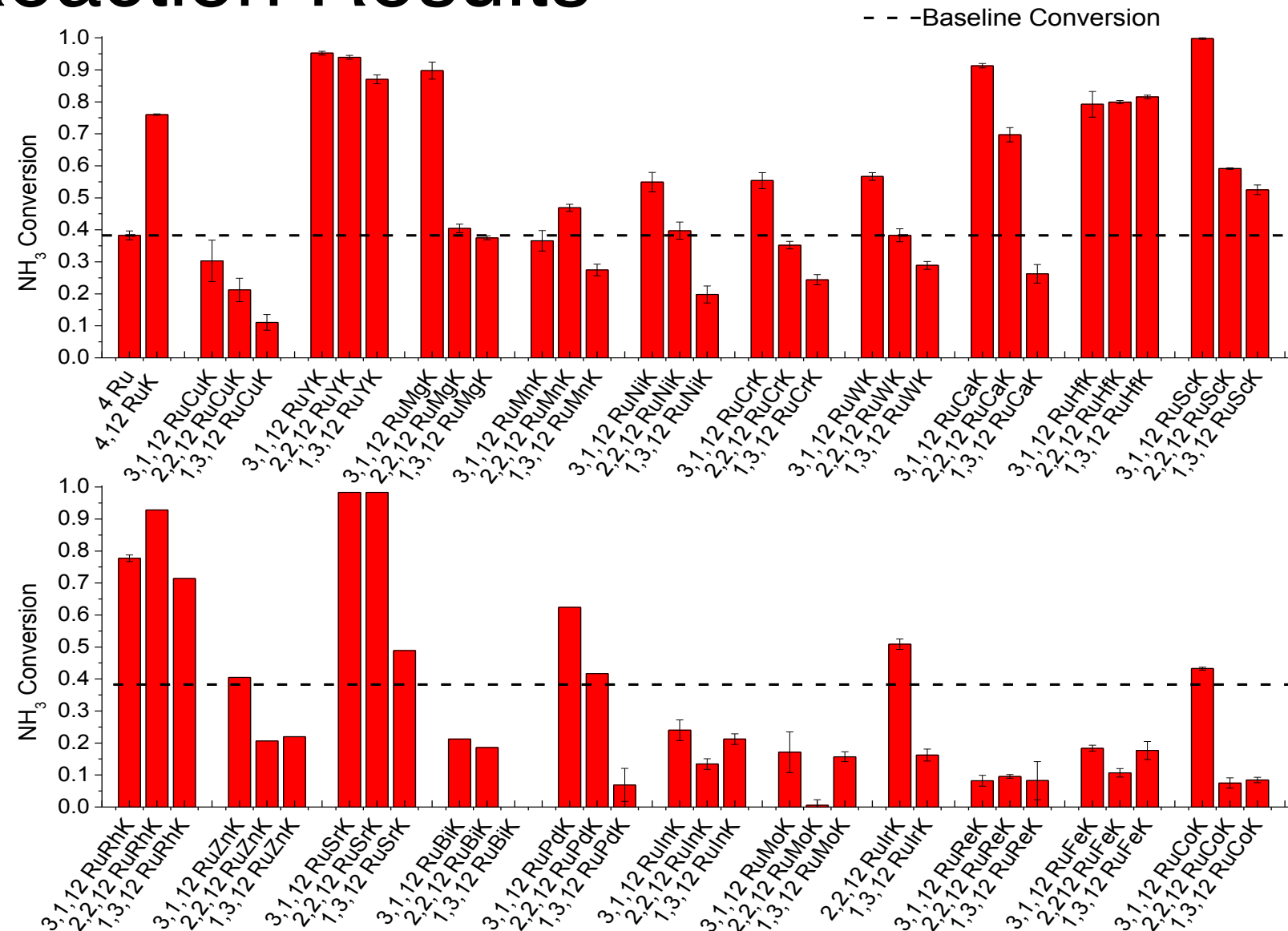
1% NH₃ in balance Ar

Pressure = 1.01 bar

200 mg catalyst

30,000 mL/g·cat ·hr

Reaction Results



Reaction Conditions

Temperature = 300°C

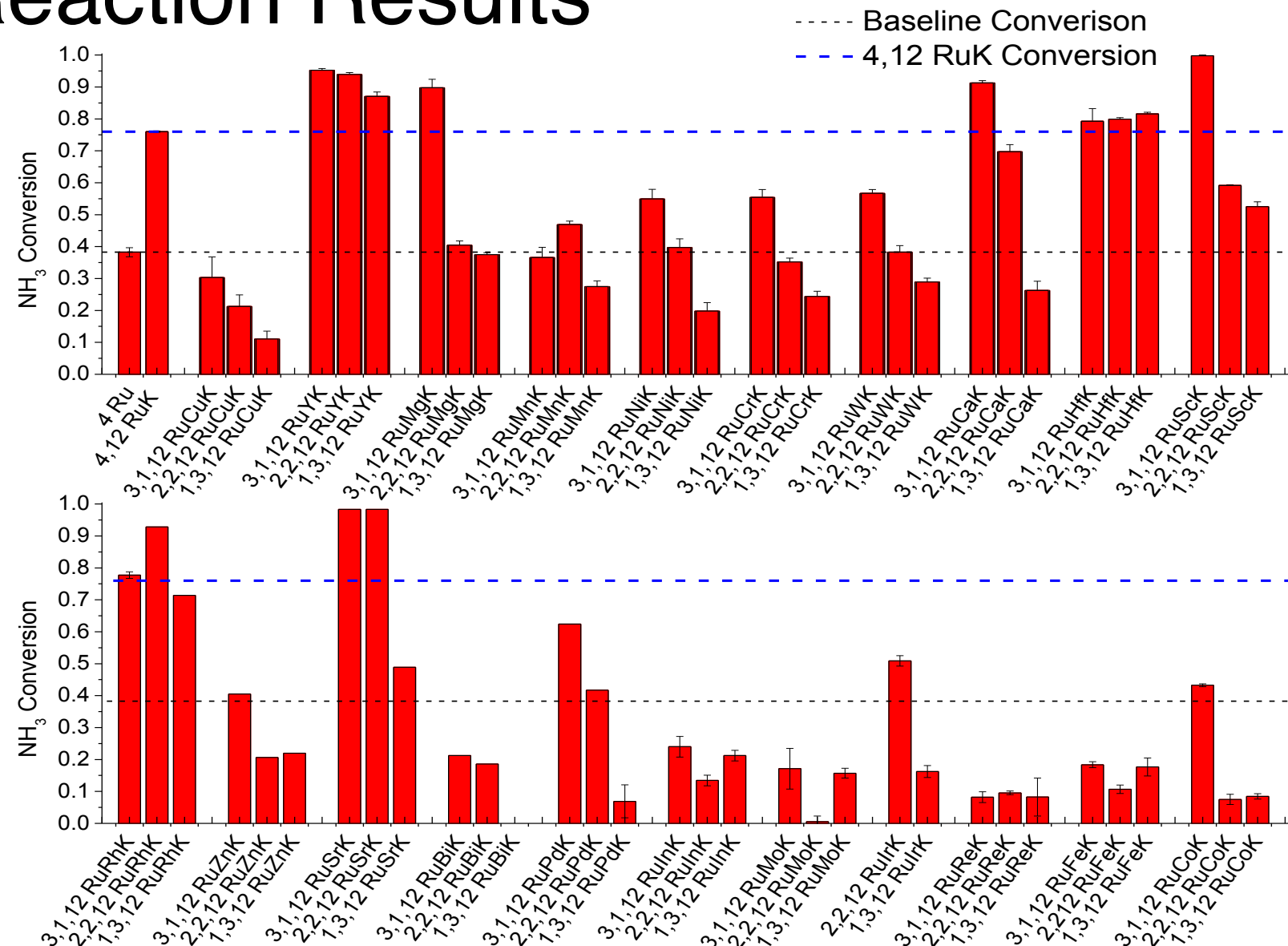
1% NH₃ in balance Ar

Pressure = 1.01 bar

200 mg catalyst

30,000 mL/g·cat · hr

Reaction Results



Reaction Conditions

Temperature = 300°C

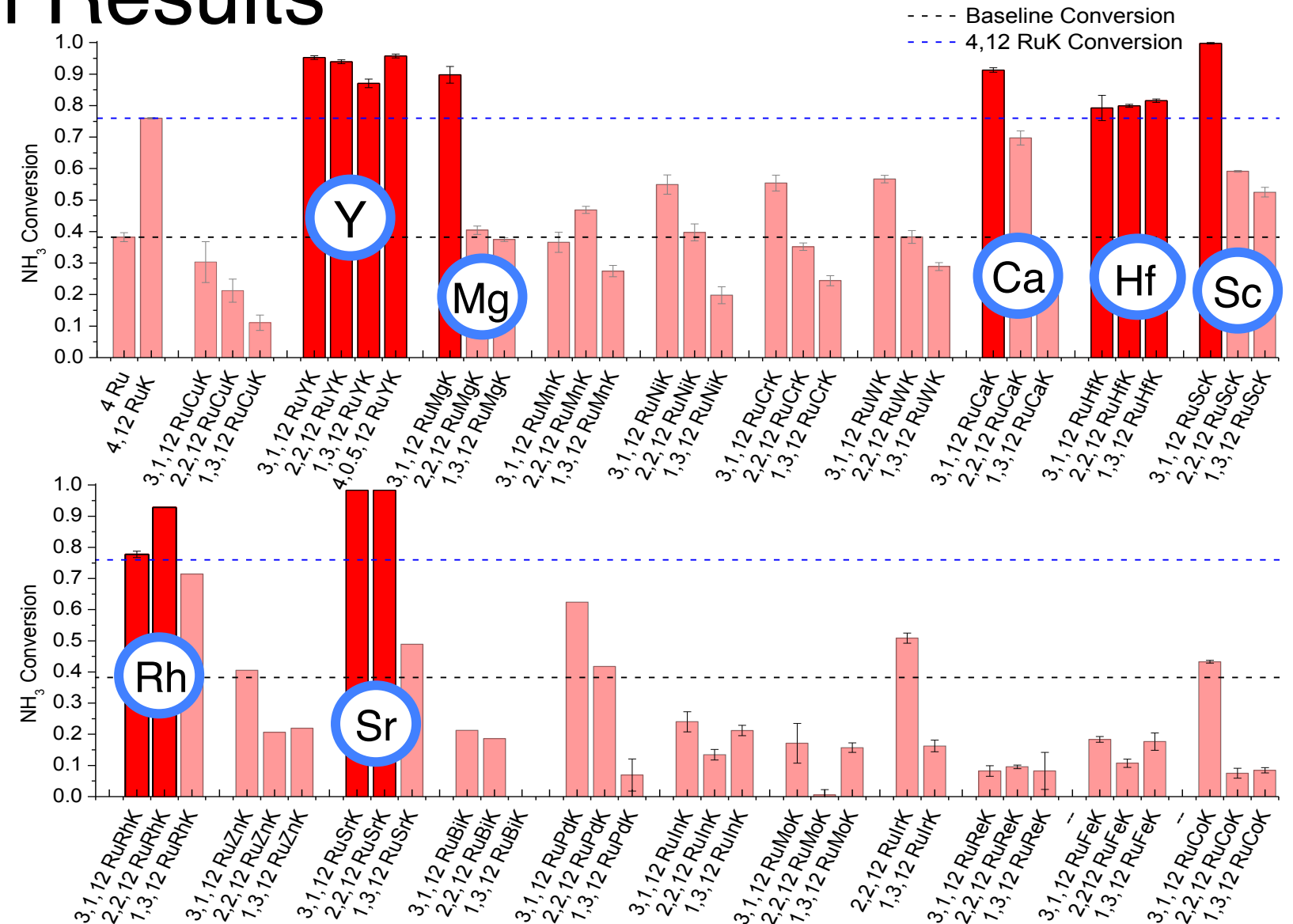
1% NH₃ in balance Ar

Pressure = 1.01 bar

200 mg catalyst

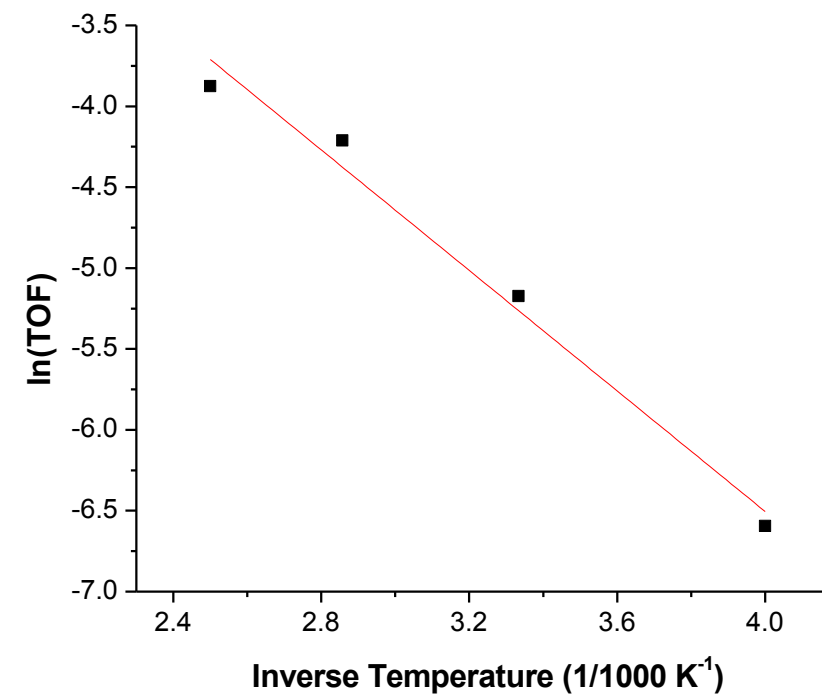
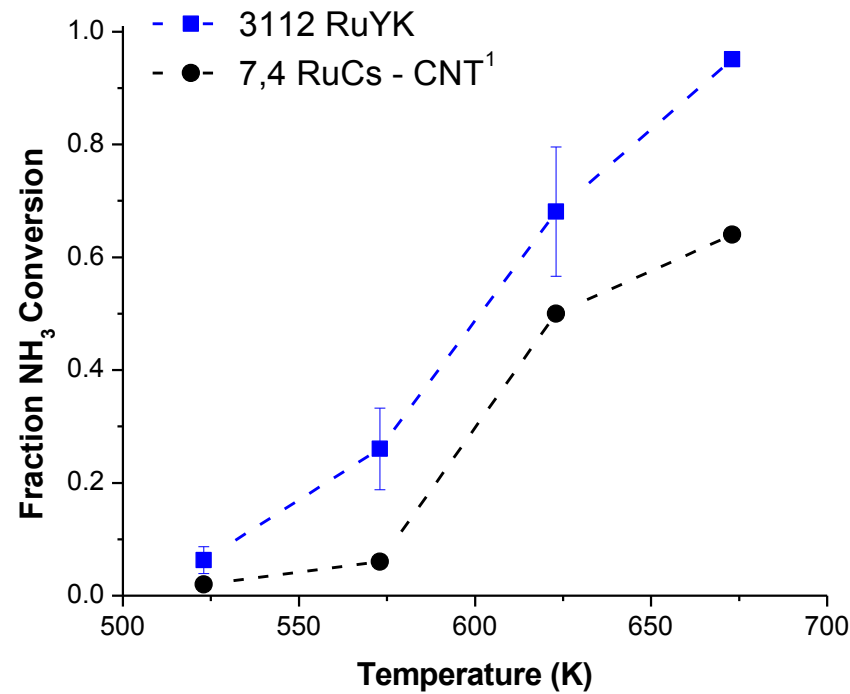
30,000 mL/g·cat ·hr

Reaction Results



Reaction Conditions: Temperature = 300°C, 1% NH_3 in balance Ar, Pressure = 1.01 bar, 200 mg catalyst, 30,000 mL/g \downarrow cat · hr

3,1,12 RuYK



Catalytic Activity in 100% NH_3 , atmospheric pressure and 52,000 mL $\text{NH}_3 \cdot (\text{min} \cdot \text{g}_{\text{cat}})^{-1}$

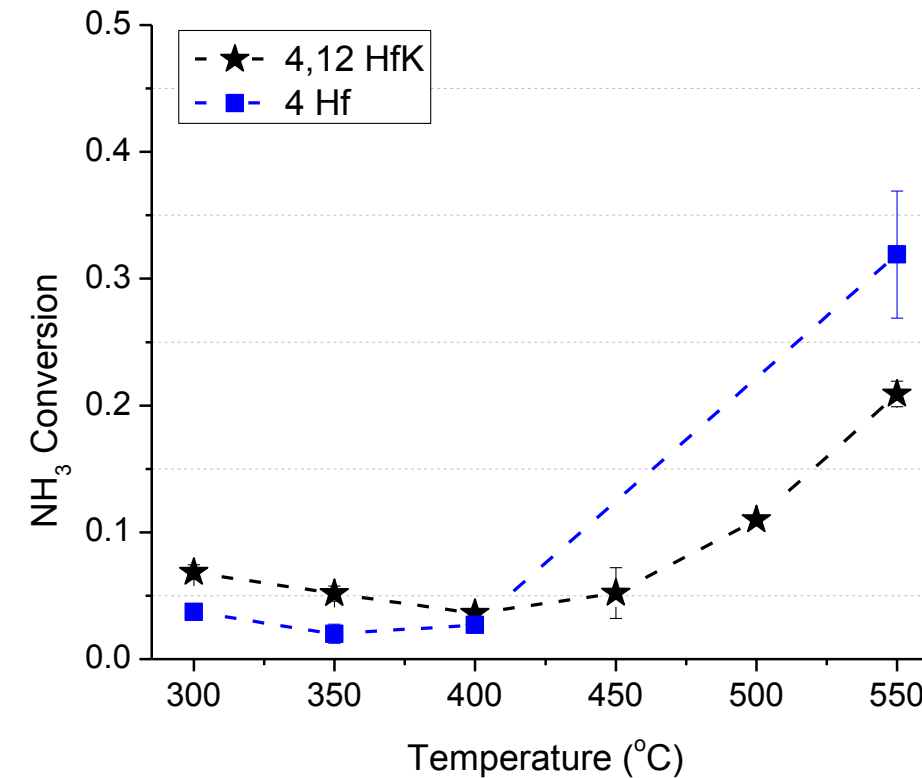
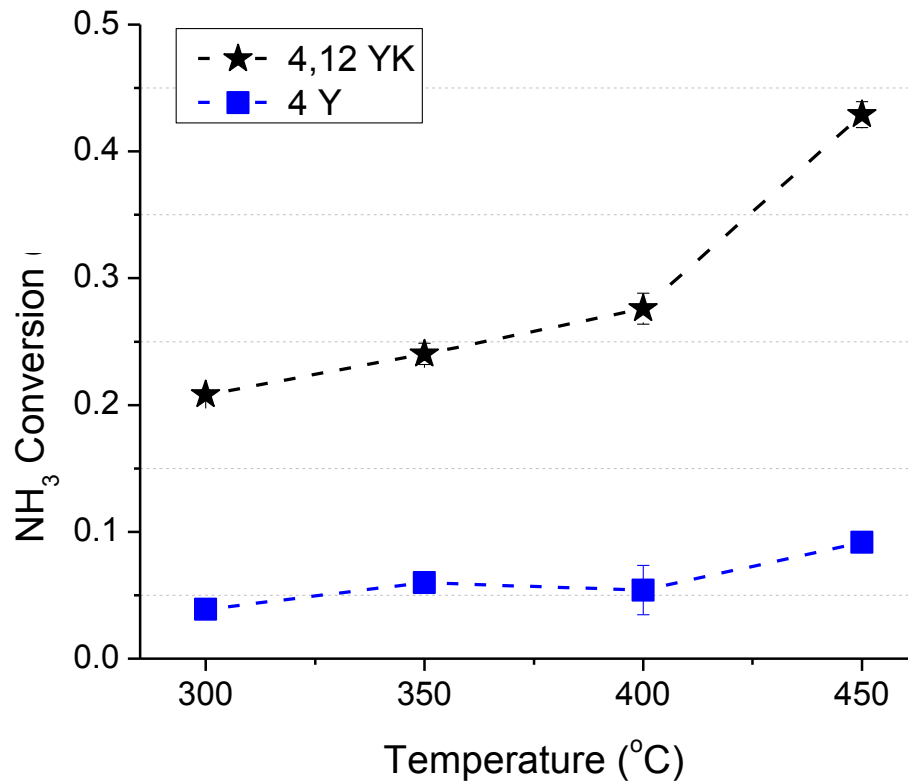
Catalyst	Conversion @ 673K	Activation Energy (kJ/mol)
3,1,12 RuYK – Al_2O_3	95	54.1
7,4 RuCs – CNT ¹	64	78.6

[1] Hill, Applied Catalysis B: Environmental 172–173, (2015), 129-135.

Mukherjee et al., Applied Catalysis B: Environmental 226 (2018) 162-181.

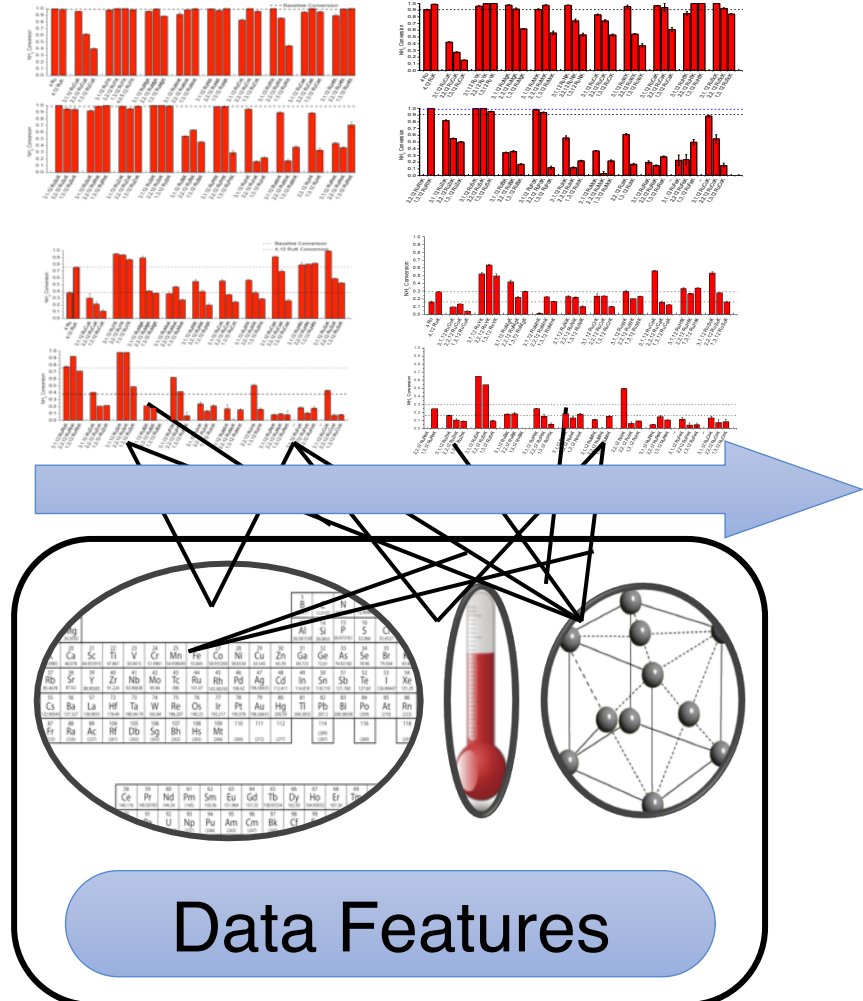
Provisional Patent Pending: "Ammonia Decomposition Catalysts and Systems", US patent application 62/720,356, August 2018.

Single Reactor Results



Reaction Conditions: 10% NH_3 in balance Ar, Pressure = 1.01 bar, 200 mg catalyst, 30,000 mL/g/cat ·hr

Application of Machine Learning in Experimental Catalysis



Machine
Learning

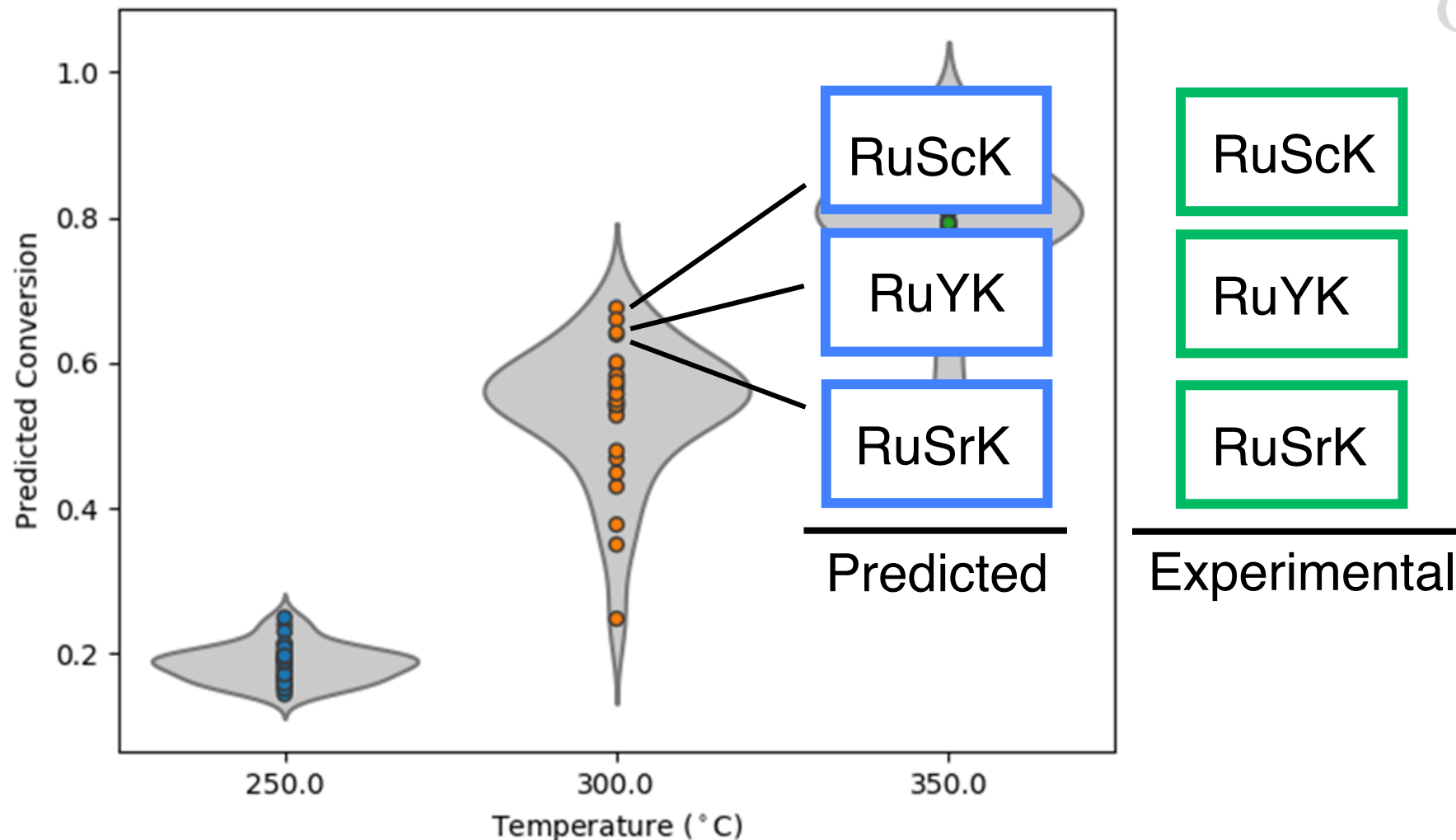
Feature Impacts

Determine which features cause better performance

Find optimally performing material faster and with less experiments

Predictions

Catalyst Predictions



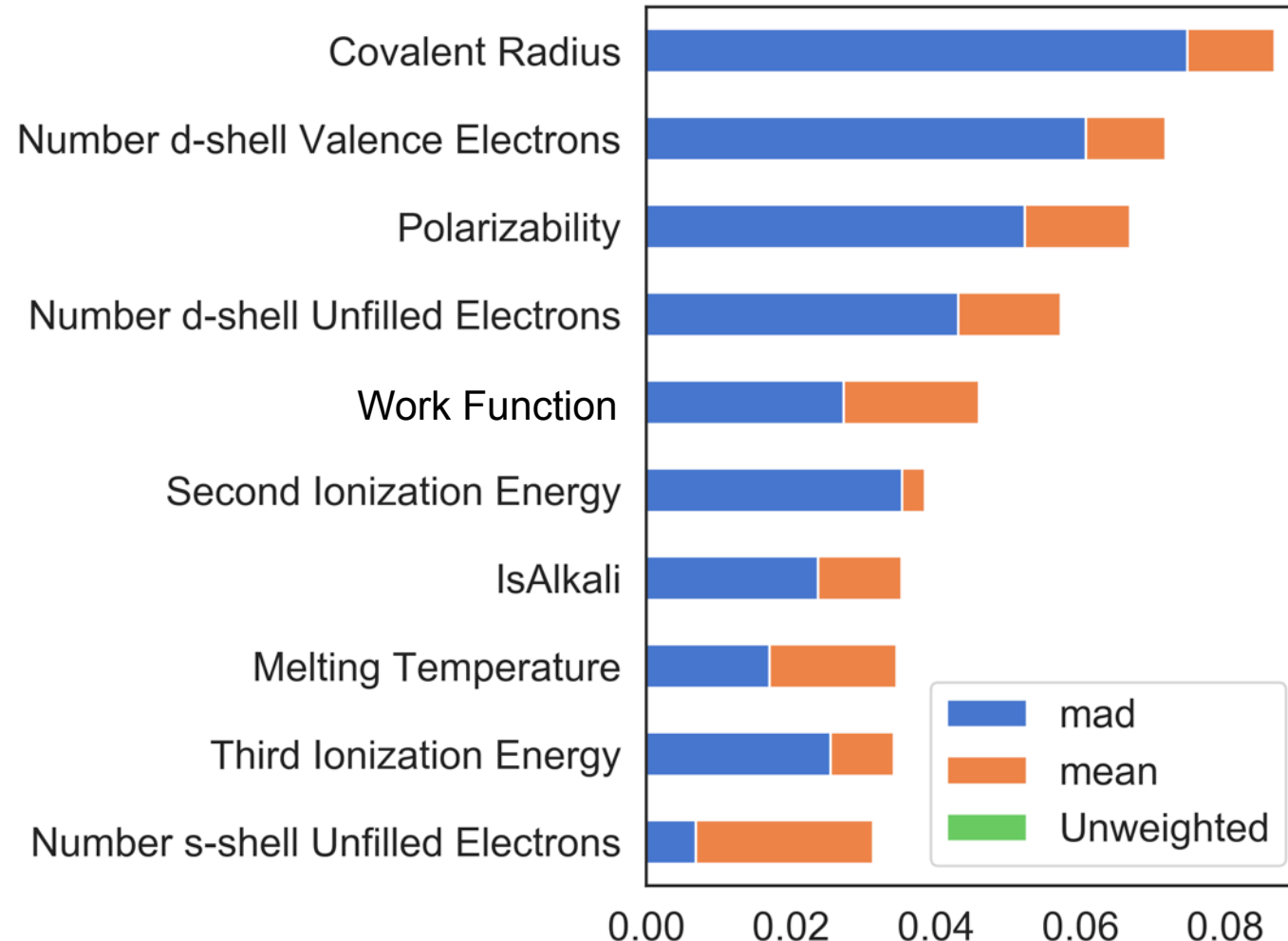
Predicted NH_3 conversion using RuCaK, RuMnK, and RuInK catalysts
tested at 250, 300, and 350°C as a training set

ML – Knowledge Extraction

Mean Absolute Deviation (MAD)

$$\sum \frac{1}{n} (x_i - \mu)$$

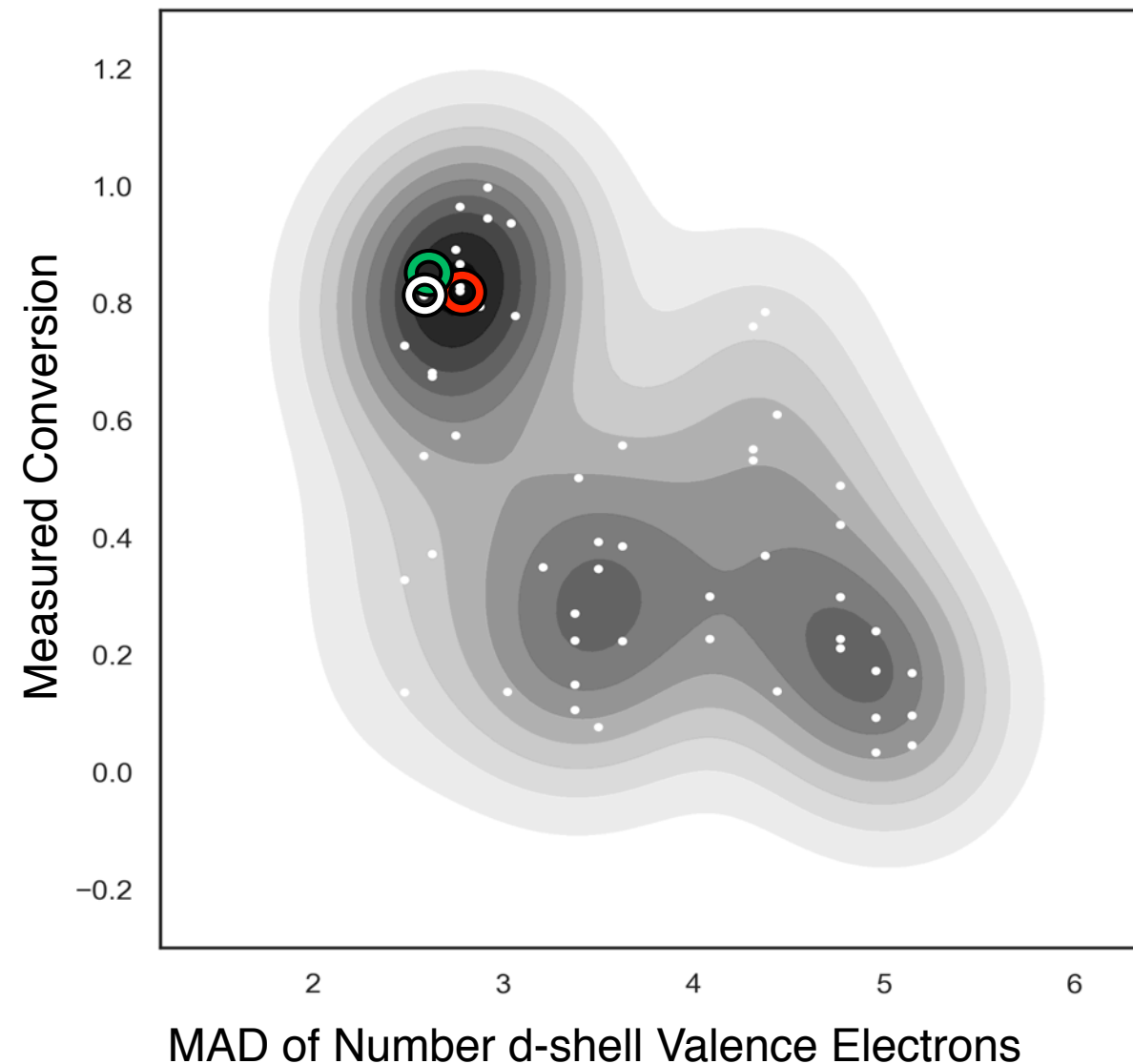
x_i = value of property
 μ = average
 n = number of samples



Number d-shell Valence Electrons

T = 300°C

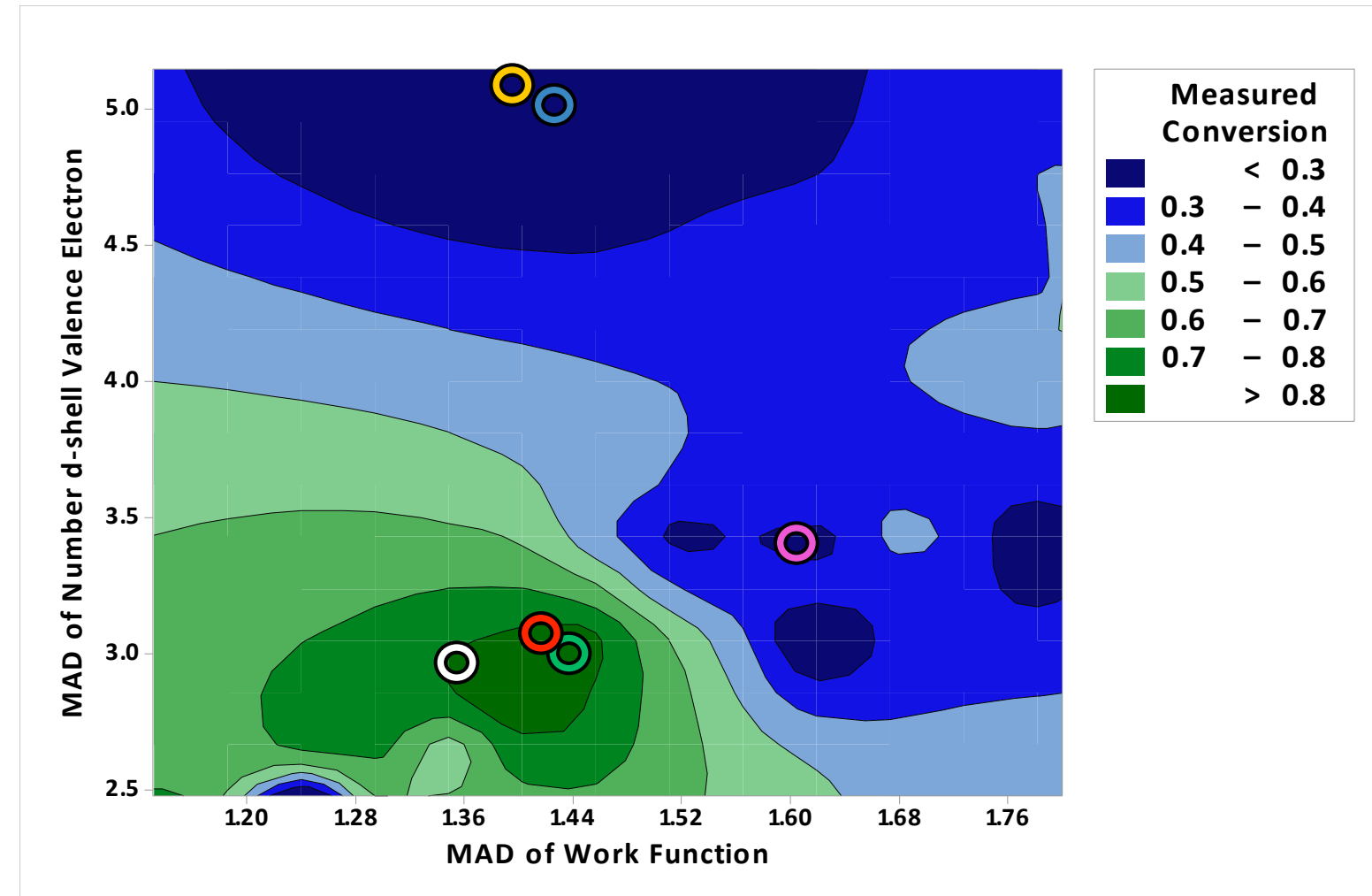
- 2212 RuYK
- 3112 RuMgK
- 3112 RuHfK



Feature Interactions

T = 300°C

- (○) 2212 RuYK
- (○) 3112 RuMgK
- (○) 3112 RuHfK
- (○) 2212 RuInK
- (○) 1312 RuZnK
- (○) 3112 RuMoK



Conclusions

- HTE allows us to screen large amounts of catalysts for low temperature NH₃ decomposition
 - New catalysts formulations discovered substituting Ru with Y and Hf
 - At 300°C, we achieved 30% higher conversion than the “state of the art” catalyst, which has more than 2x Ru
- ML allows to unravel important factors and interactions from HTE data
 - Extraction of features
 - Systematic trends from feature interactions
- Guide future iterations of catalyst design

Acknowledgements



- Strategic Approach to the Generation of Electricity Center (SAGE)
- NSF IGERT DGE-1250052
- ARPA-E DE-AR0000931
- Travis Williams
 - Data Science in Catalysis
 - Nov 1 @ 12:30pm Rm 402



CHANGING WHAT'S POSSIBLE

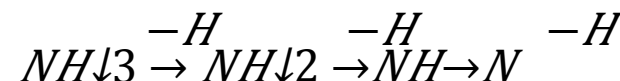


Supplemental Slides

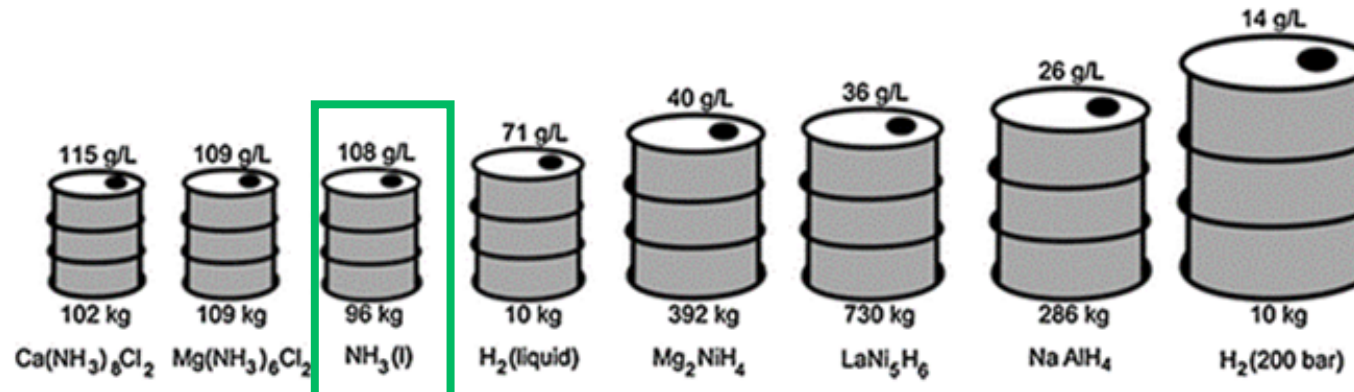
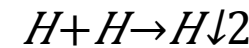
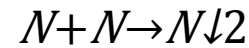
Ammonia Decomposition

- Efficient method for hydrogen storage and transportation
- Liquid at 8 bar and 298K
- Less volume and weight than alternative hydrogen storage methods

Dehydrogenation



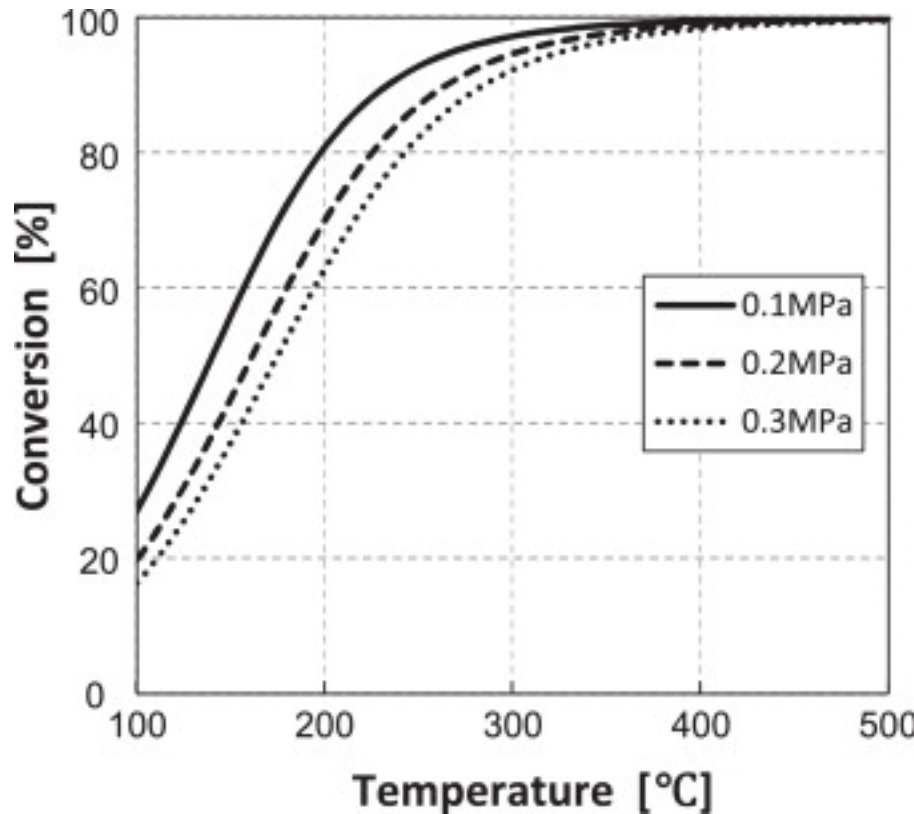
Recombination



Comparison of equivalent mass and volume of 10 kg of hydrogen stored in different materials

Ammonia Decomposition

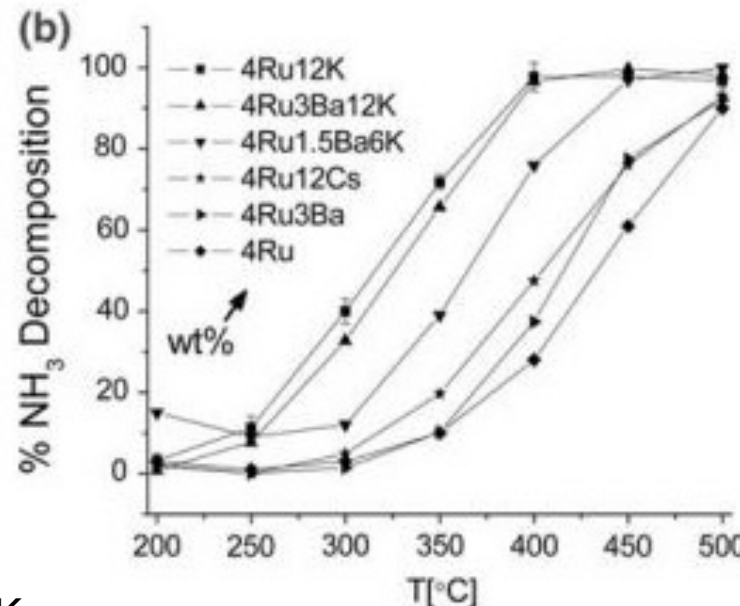
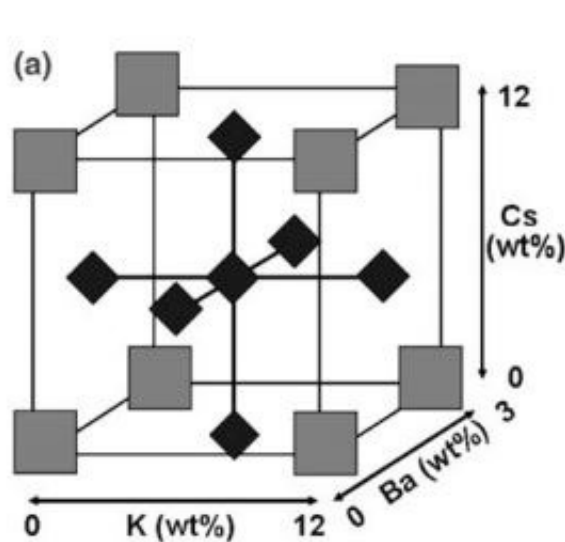
Ru supported catalysts



- 100% conversion at 823K (550°C)
- >95% conversion at low temperatures to avoid degradation of fuel cell

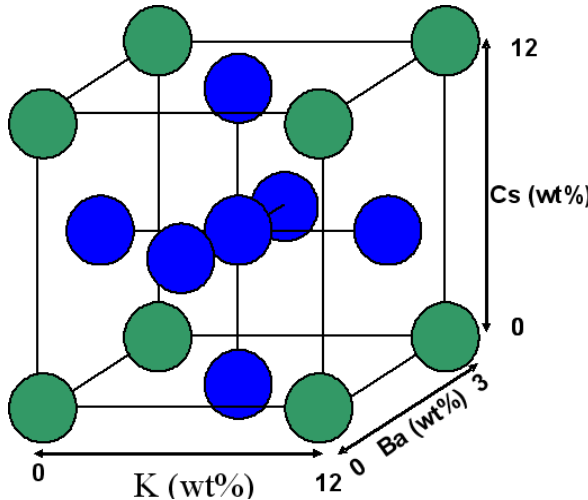
Ammonia Decomposition Promoters

- Tested K, Cs, Ba, Sr, Rb, Ca, Na and Li
- K, Cs and Ba loadings optimized through a surface response study
- Developed response surface model as a function of promoters
- Promotional effects completely dominated by K



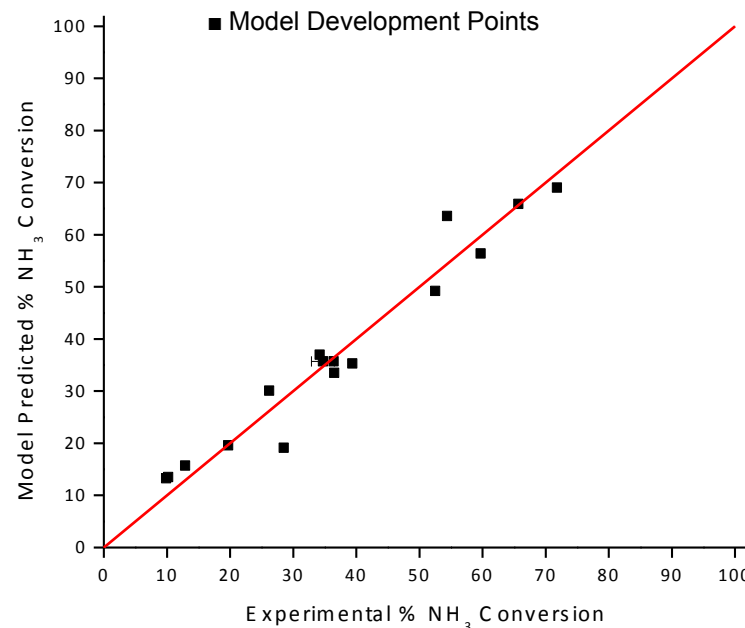
Response surface model for Ba/Cs/K promoters on 4wt%Ru on Al_2O_3

Promotion of Ru/ γ -Al₂O₃ Catalysts



Term	Coefficients
Constant	35.7
Ba	-1.8
K	22.3
Cs	-2.6
Ba*Ba	-0.5
K*K	5.6
Cs*Cs	-3.0
Ba*K	-0.9
Ba*Cs	-1.0
K*Cs	-4.7

$$R = C + \alpha_1(Ba) + \alpha_2(K) + \alpha_3(Cs) + \dots + \beta_1(Ba)^2 + \beta_2(K)^2 + \dots + \lambda_1(Ba*K) + \lambda_2(Ba*Cs) + \dots$$



Carbon Free Hydrogen Storage and Generation materials

Metal Hydrides

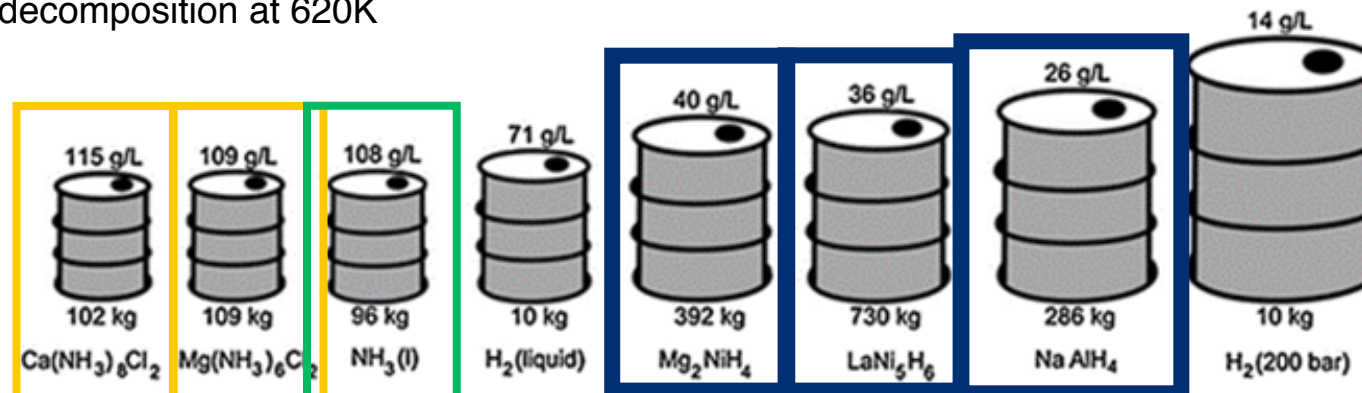
- NaAlH_4 - 5.6% H_2 but needs 10-40MPa to dehydrogenate
- LaNi_5H_6 - 1.37% H_2
- MgNiH_4 - 3.59% H_2

Ammonia

- 17.4 wt% H_2
- Liquefied at RT and 8 bar
- Established transportation infrastructure and safety precautions

Metal Amines

- Metal chlorides easily complex with amines
- $\text{Mg}(\text{NH}_3)_6\text{Cl}_2$
- Complete decomposition at 620K

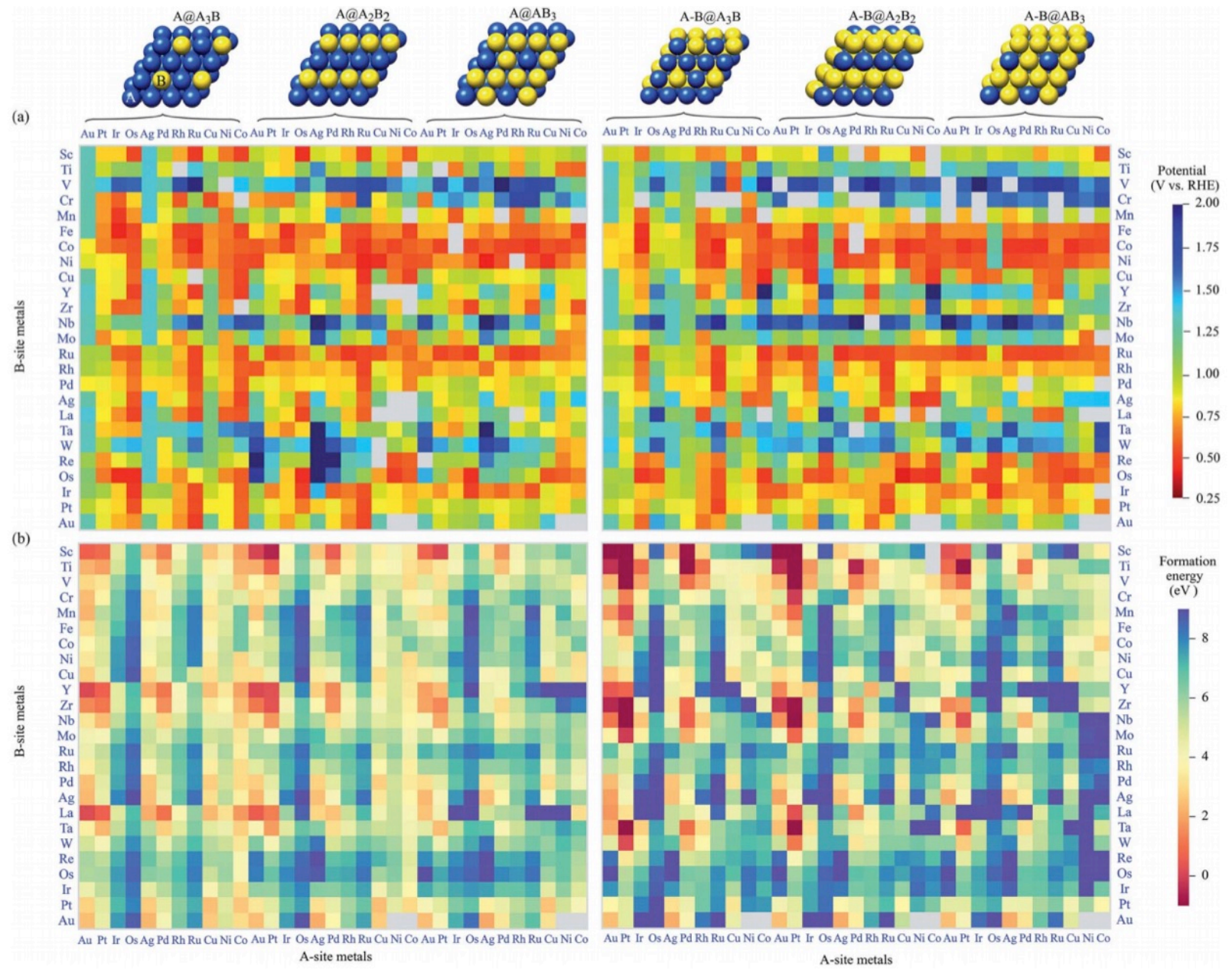


Comparison of equivalent mass and volume of 10 kg of hydrogen stored in different materials

Sakintuna B., Internation Journal of Hydrogen Energy. (2007). 32:1121-1140.

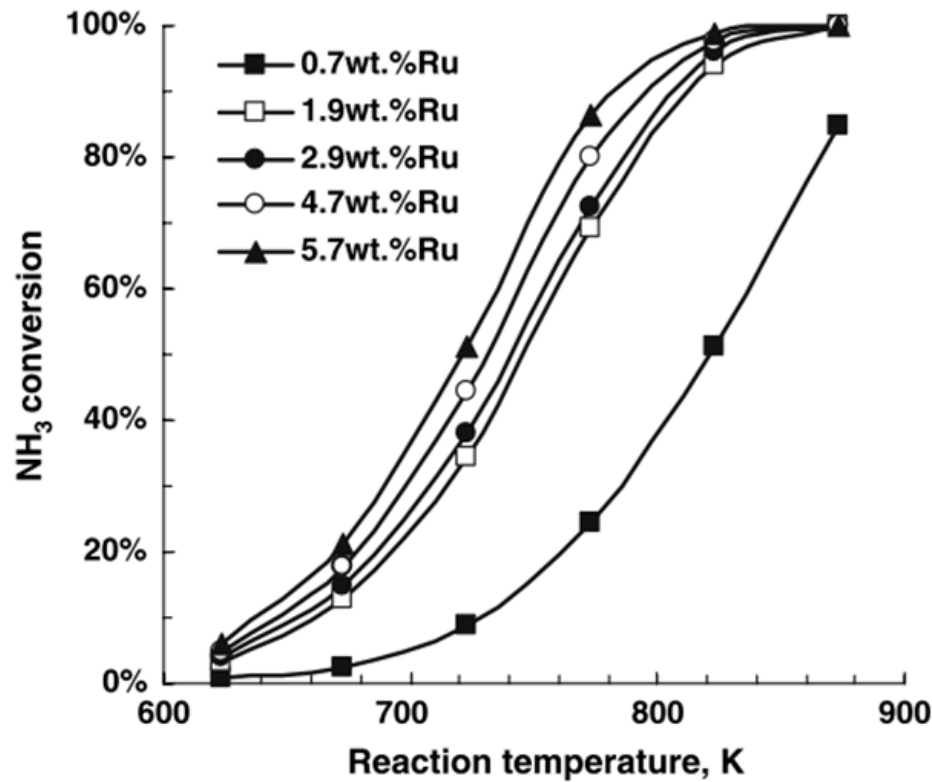
Christensen et al., Journal of Materials Chemistry. (2005) 15:4106-4107.

Mukherjee et al., Applied Catalysis B: Environmental 226 (2018) 162-181.



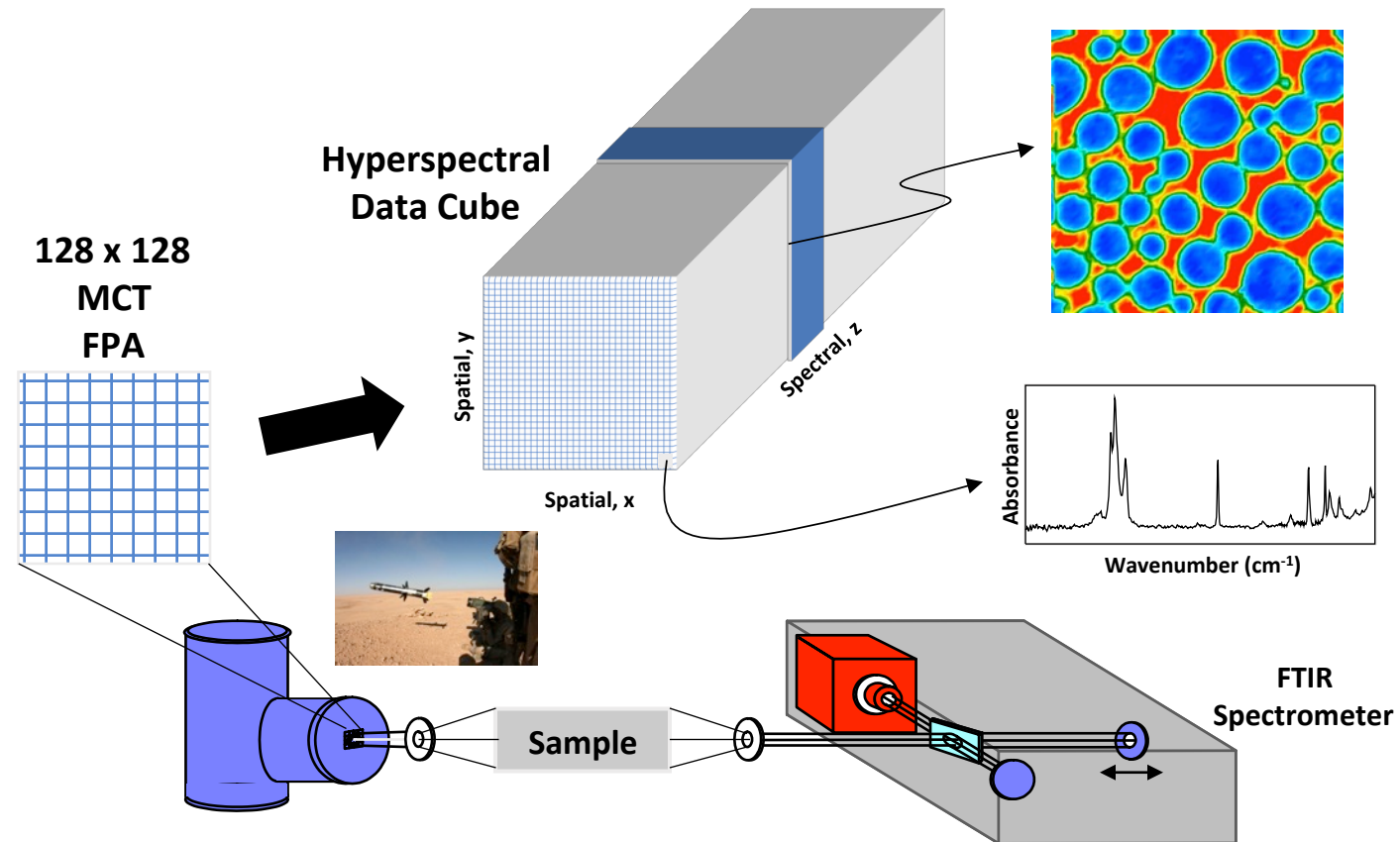
Ammonia Decomposition

Particle Size and Morphology



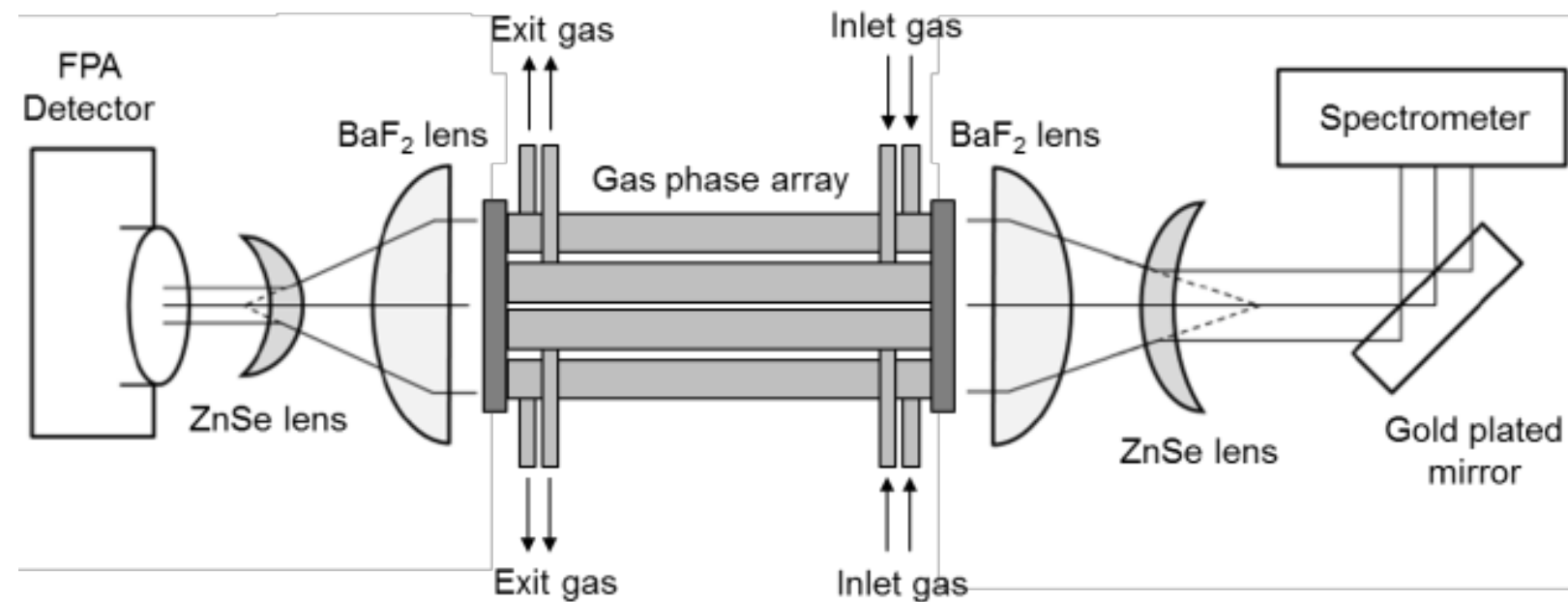
Ru wt%	0.7	1.9	2.9	4.7	5.7
Mean particle size (TEM)	1.9	2.2	2.9	3.5	4.2

FTIR Imaging



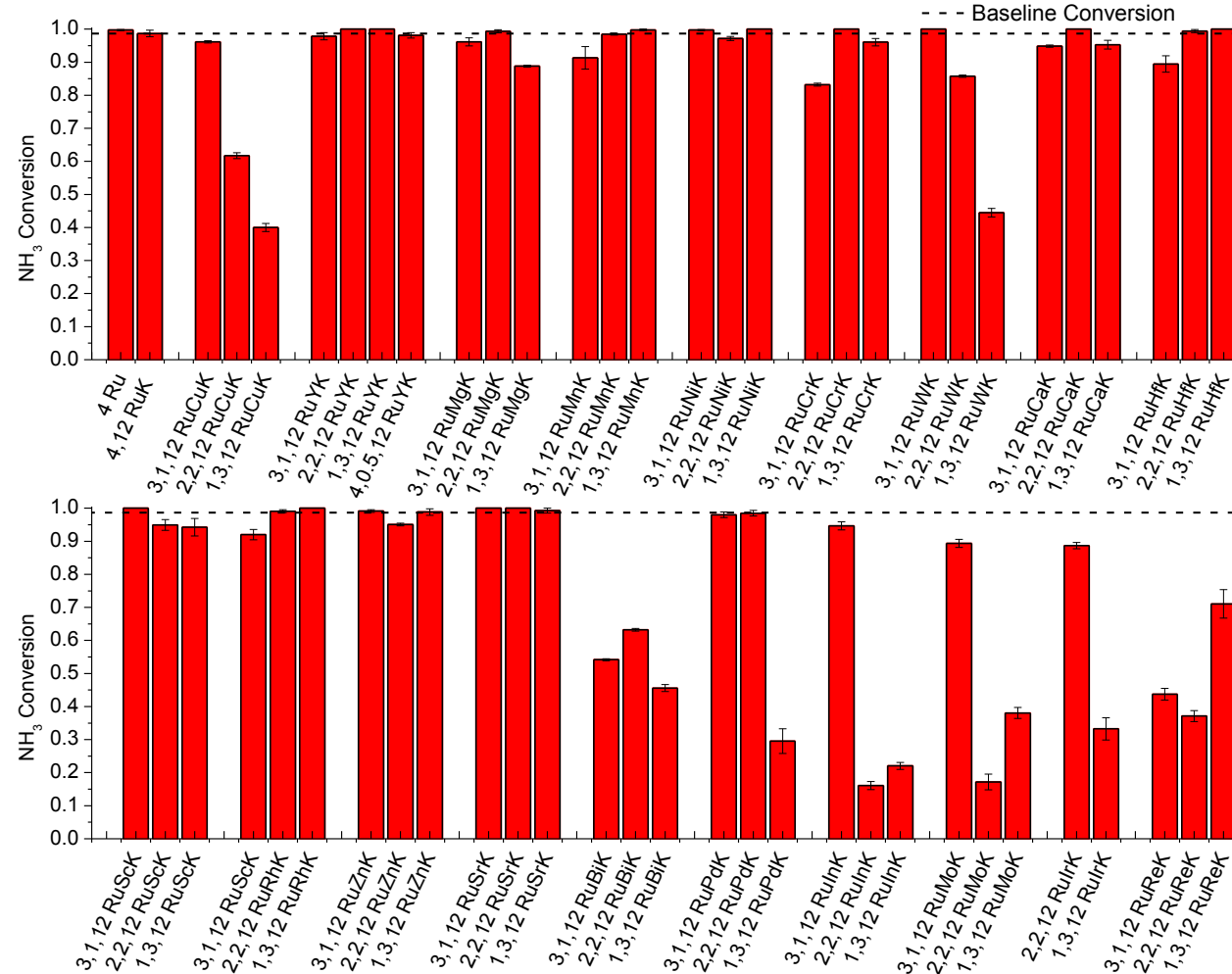
Snively, C.M. and J. Lauterbach *Applied Spectroscopy* 59(2005)

Parallel FTIR Imaging



Reaction Results

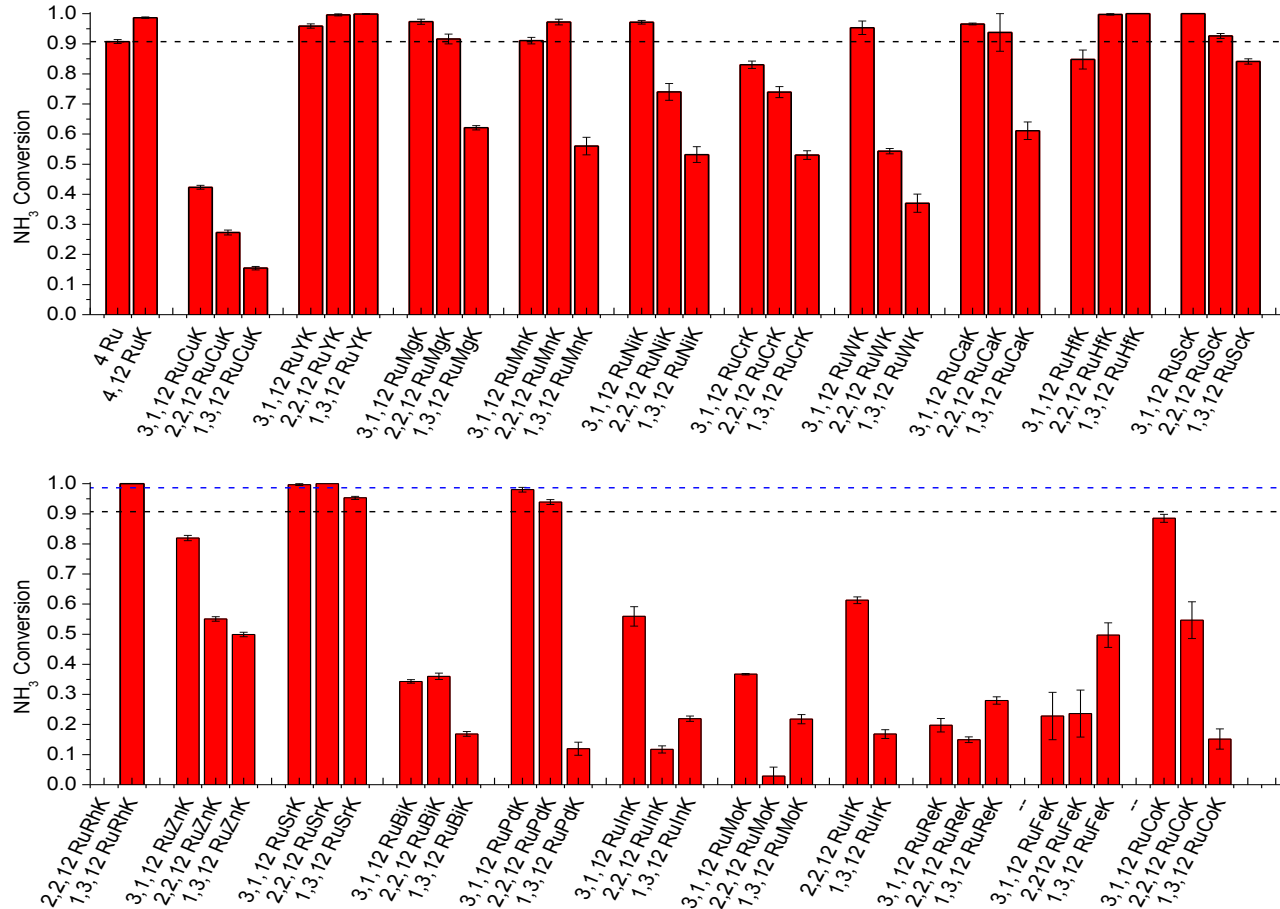
T = 400°C



Reaction Conditions: 1% NH₃ in balance Ar, Pressure = 1.01 bar, 200 mg catalyst, 30,000 mL/g↓cat
 ·hr

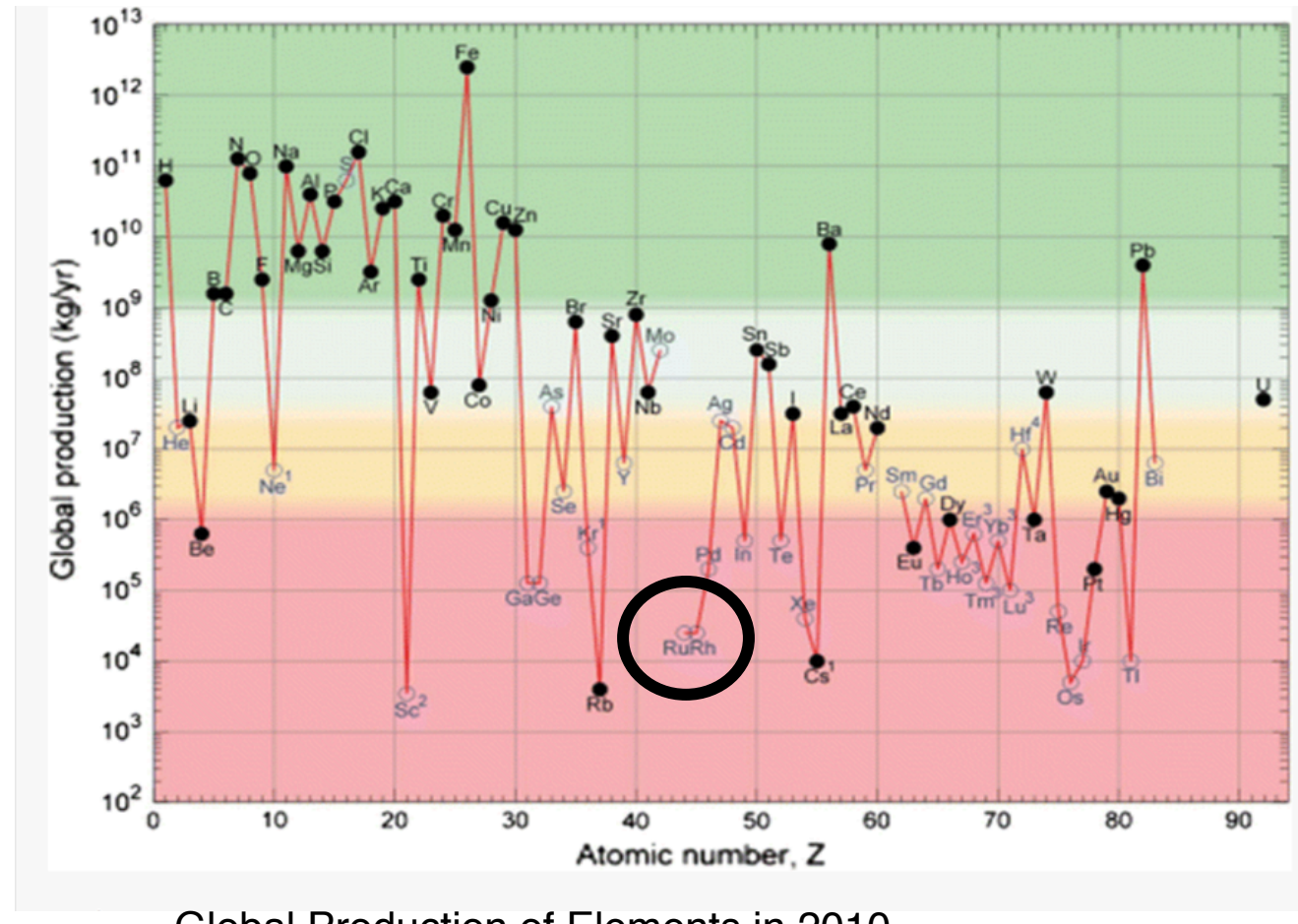
Reaction Results

T = 350°C



Reaction Conditions: 1% NH₃ in balance Ar, Pressure = 1.01 bar, 200 mg catalyst, 30,000 mL/g $\sqrt{\text{cat}} \cdot \text{hr}$

Ammonia Decomposition



Substitutional Metals for Low T Ammonia Decomposition

Promising Ru Substitutes

- Hf • Sc
- Mg • Rh
- Ca • Sr
- Mn • Y

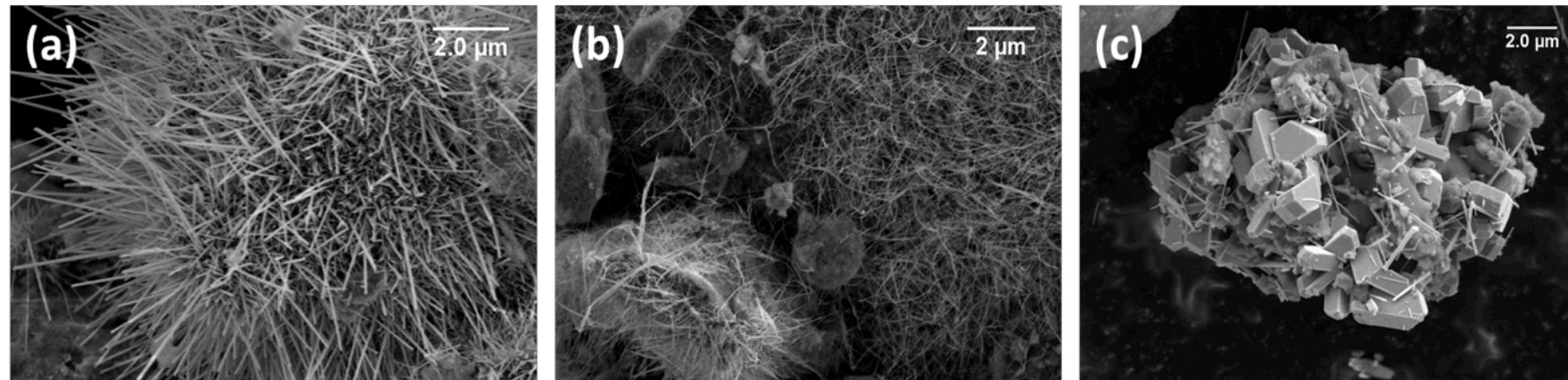
Global Production 2010

kg/yr	Ru	Hf	Mg	Ca	Sc	Sr	Rh	Y	Mn
	10⁴	10 ⁷	10 ¹⁰	10 ¹¹	10 ³	10 ⁹	10 ⁴	10 ⁷	10 ¹⁰

Price of Metal 2018

Au USD/g	Ru	Hf	Mg	Ca	Sc	Sr	Rh	Y	Mn
5.54	14.0	1.20	.003	.20	14.0	1.0	130.0	4.30	.065

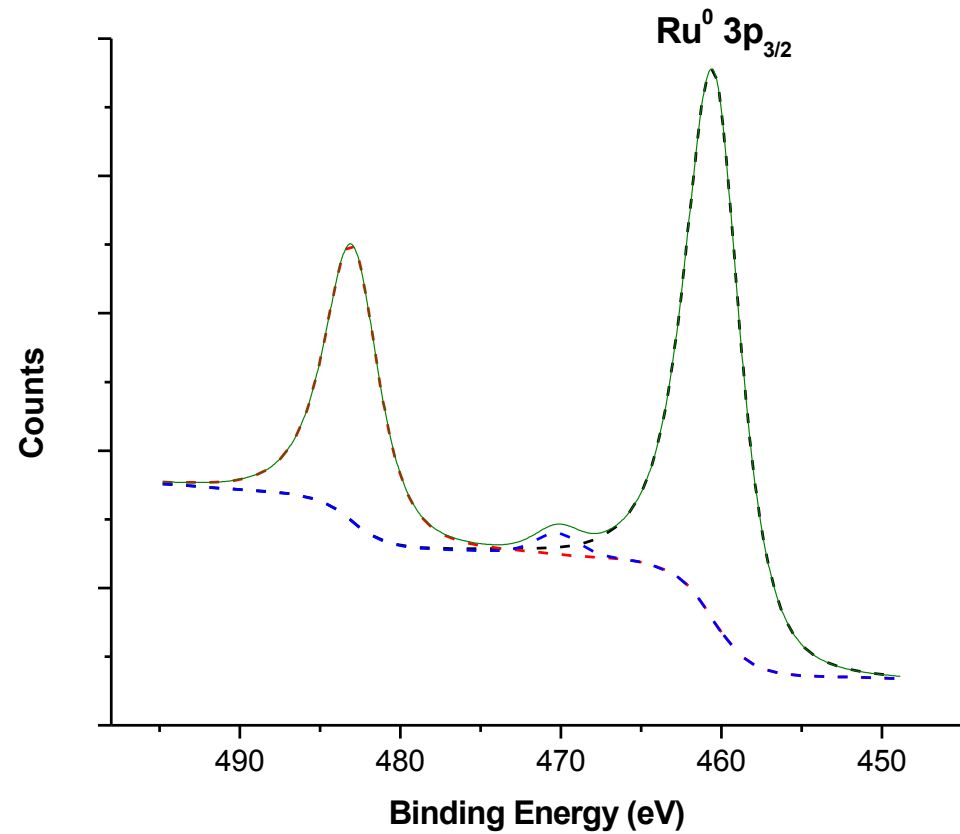
Unknown Structures



(a) 2,2,12 RuFeK **(b)** 2,2,12 RuIrK **(c)** 2,2,12 RuCoK

- Defect density is increased from decomposition of needle like precursor state, increasing catalytic activity over the nanoparticle counterparts

XPS 4,12 RuK Hollandites



4,12 RuK Hollandite XPS after
reduction in H_2 for 1hr at 450°C

Ru^0 Binding Energy (eV)	$3p_{3/2}$	$3p_{1/2}$
Reference	462.0	484.0
Actual	462.1	484.1

Machine Learning Features

Elemental Properties

- Atomic Number
- Atomic Volume
- Atomic Weight
- Boiling Temperature
- Column - Periodic Table
- Conductivity
- Covalent Radius
- Density
- Dipole Polarizability
- Electron Affinity
- Electronegativity
- Fusion Enthalpy
- Ground State Bandgap
- Ground State Energy
- Heat Capacity
- Heat of Fusion
- 1st – 8th Ionization Energy
- Melting Temperature
- Mendeleev Number
- Polarizability
- Row – Periodic Table
- Work Function

Electron Properties

- Number s-shell valance electrons
- Number p-shell valance electrons
- Number d-shell valance electrons
- Number f-shell valance electrons
- Number unfilled s-shell valance electrons
- Number unfilled p-shell valance electrons
- Number unfilled d-shell valance electrons
- Number unfilled f-shell valance electrons
- Total number valence electrons
- Total number unfilled electrons

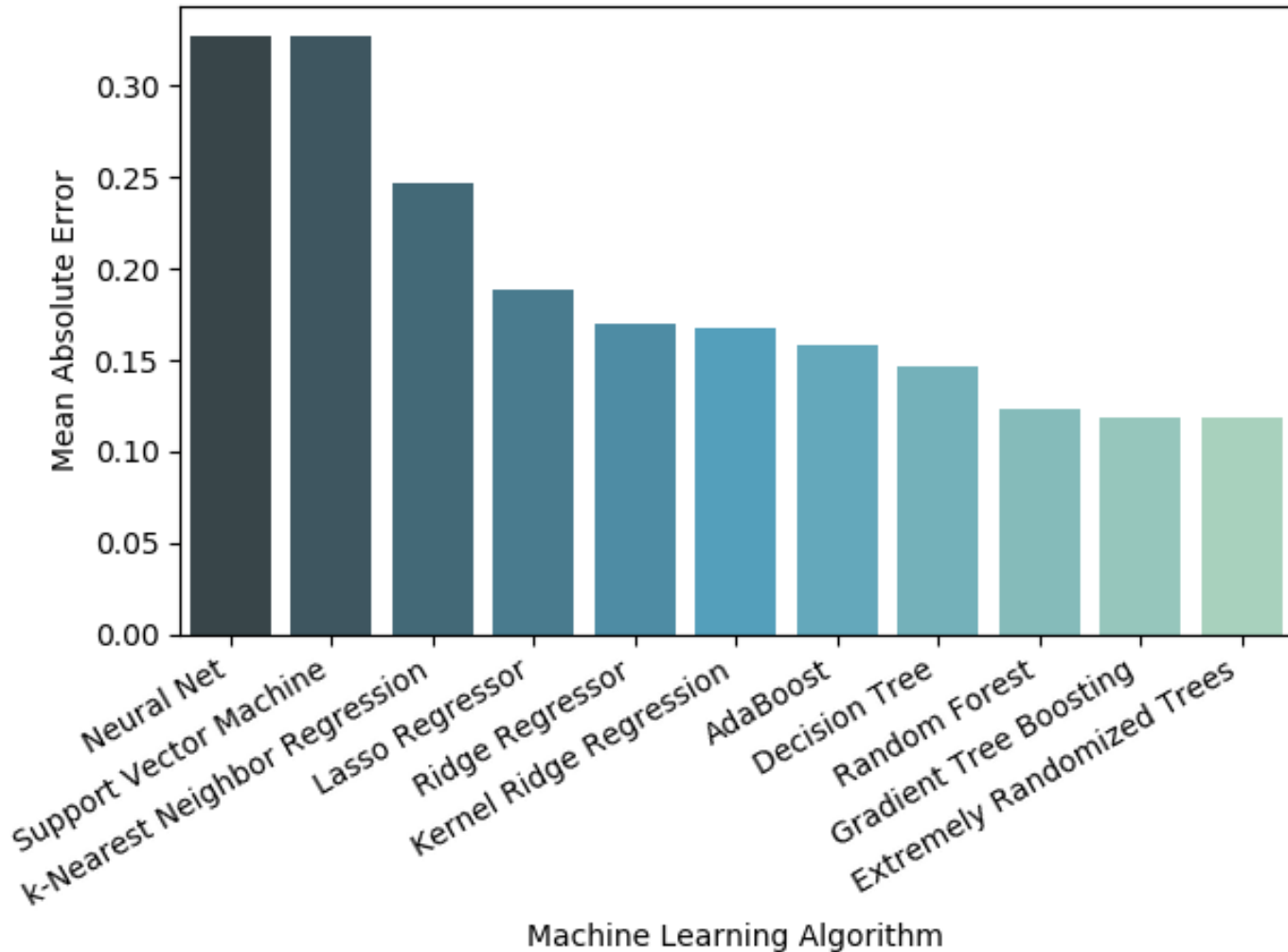
Binary Properties

- Is Alkali metal?
- Is metal?
- Is metalloid?
- Is nonmetal?
- Is d block?
- Is f block?

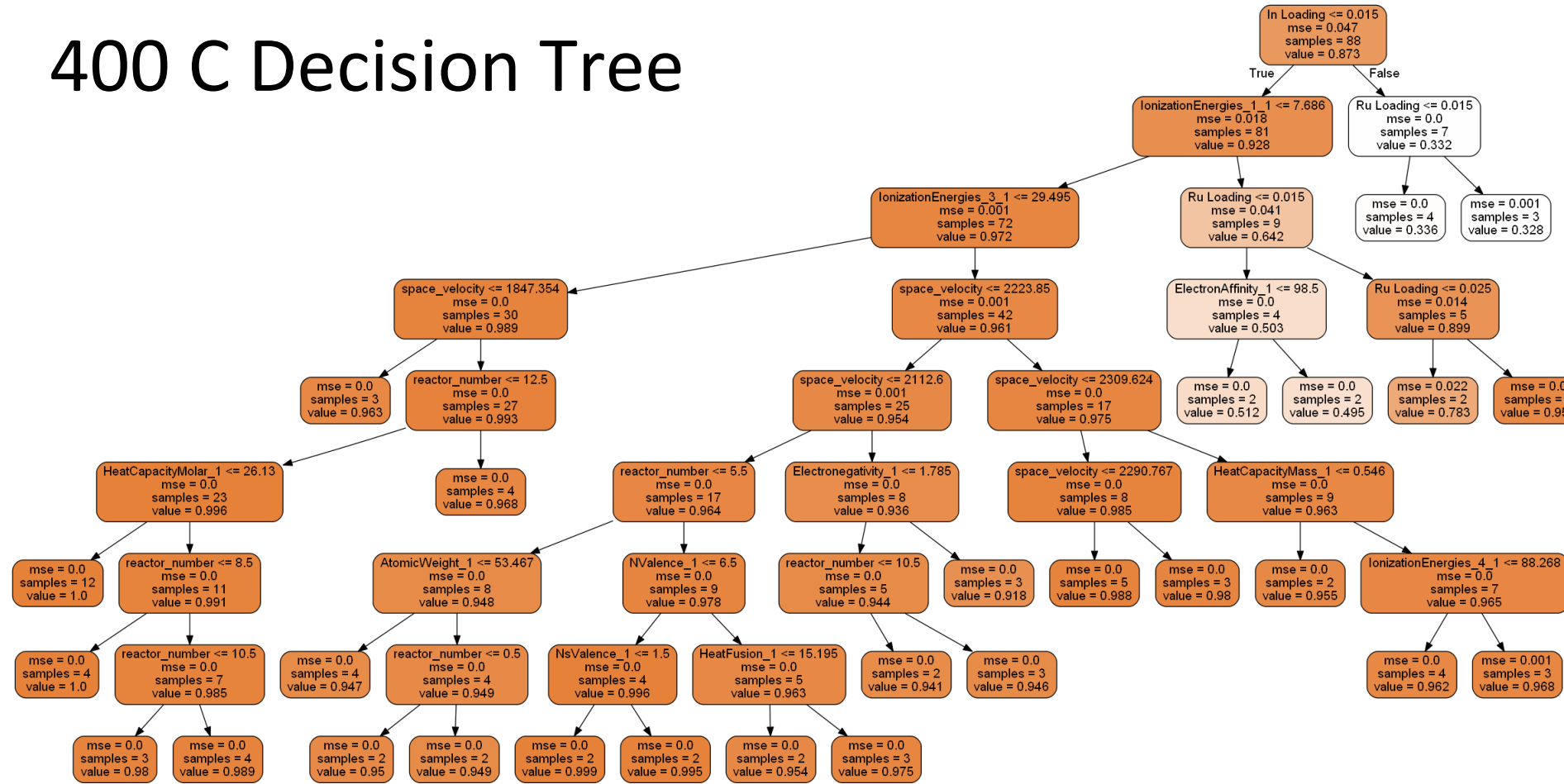
Other Properties

- Weight Loadings
- Reaction Temperature
- Space Velocity
- # of precursor Cl ligands

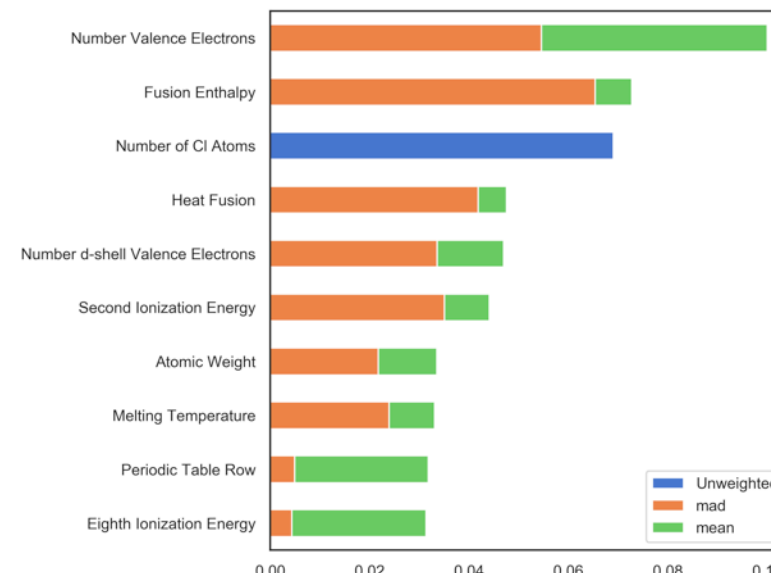
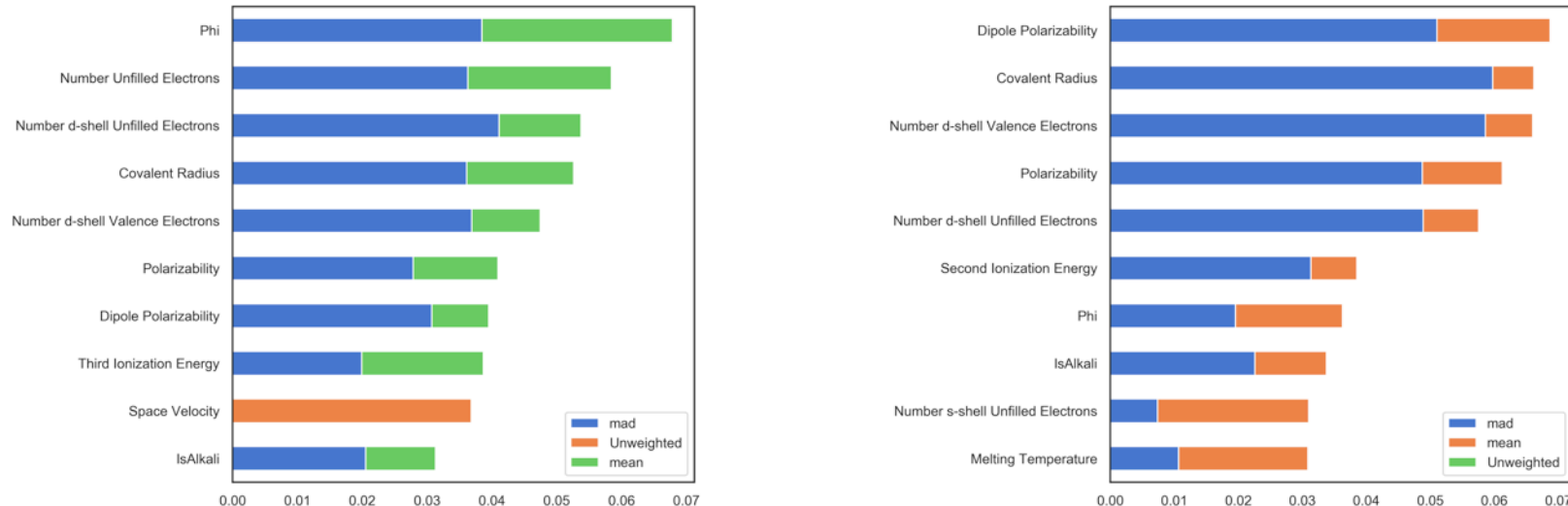
Algorithm Selection



400 C Decision Tree



Feature Importance T slices



Feature Trends

T = 300°C

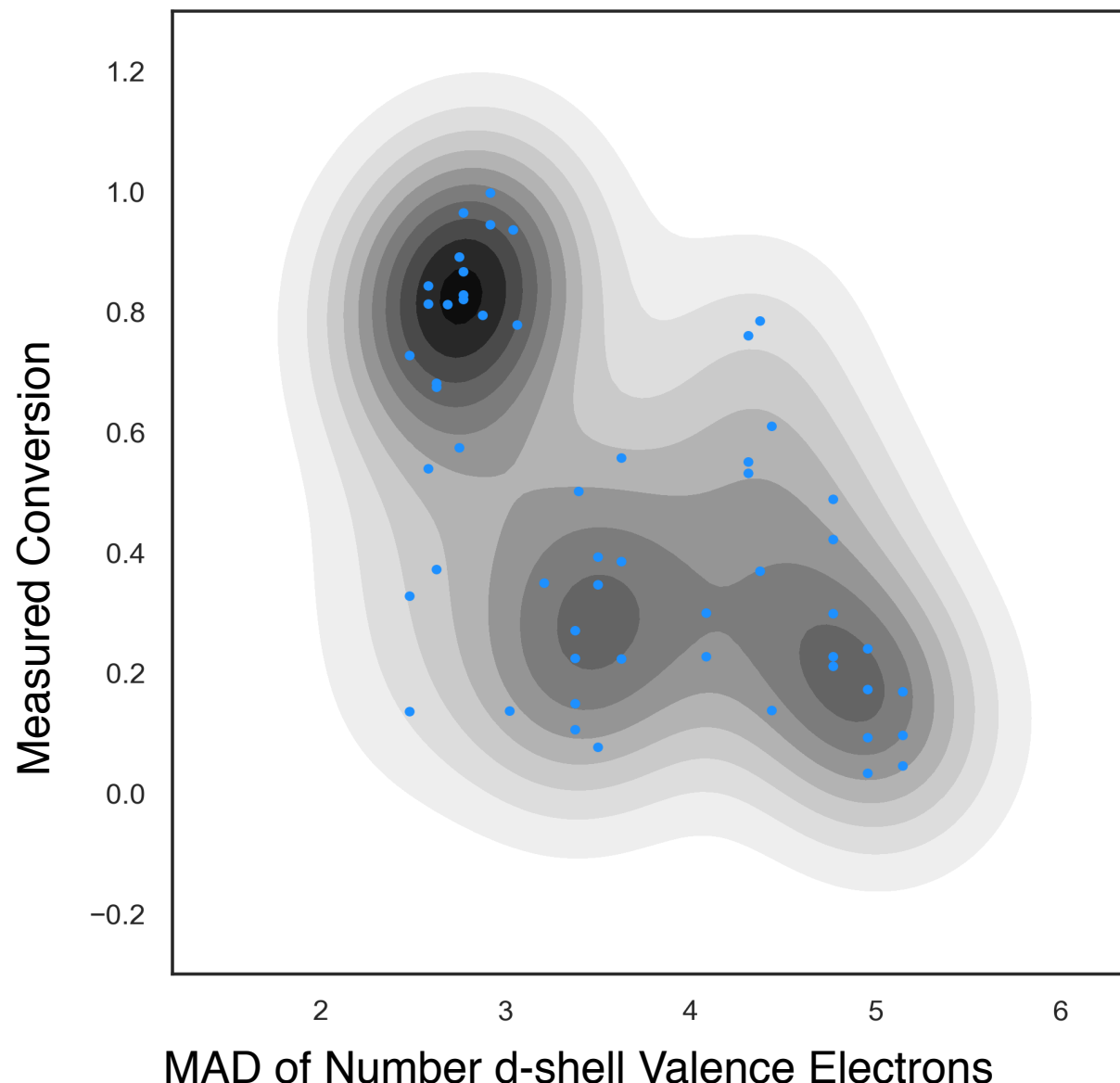
Mean Absolute Deviation (MAD)

$$\sum \frac{1}{n} (x_i - \mu)$$

x_i = value of property

μ = average

n = number of samples



Feature Interaction

T = 300°C

(○) 2212 RuYK

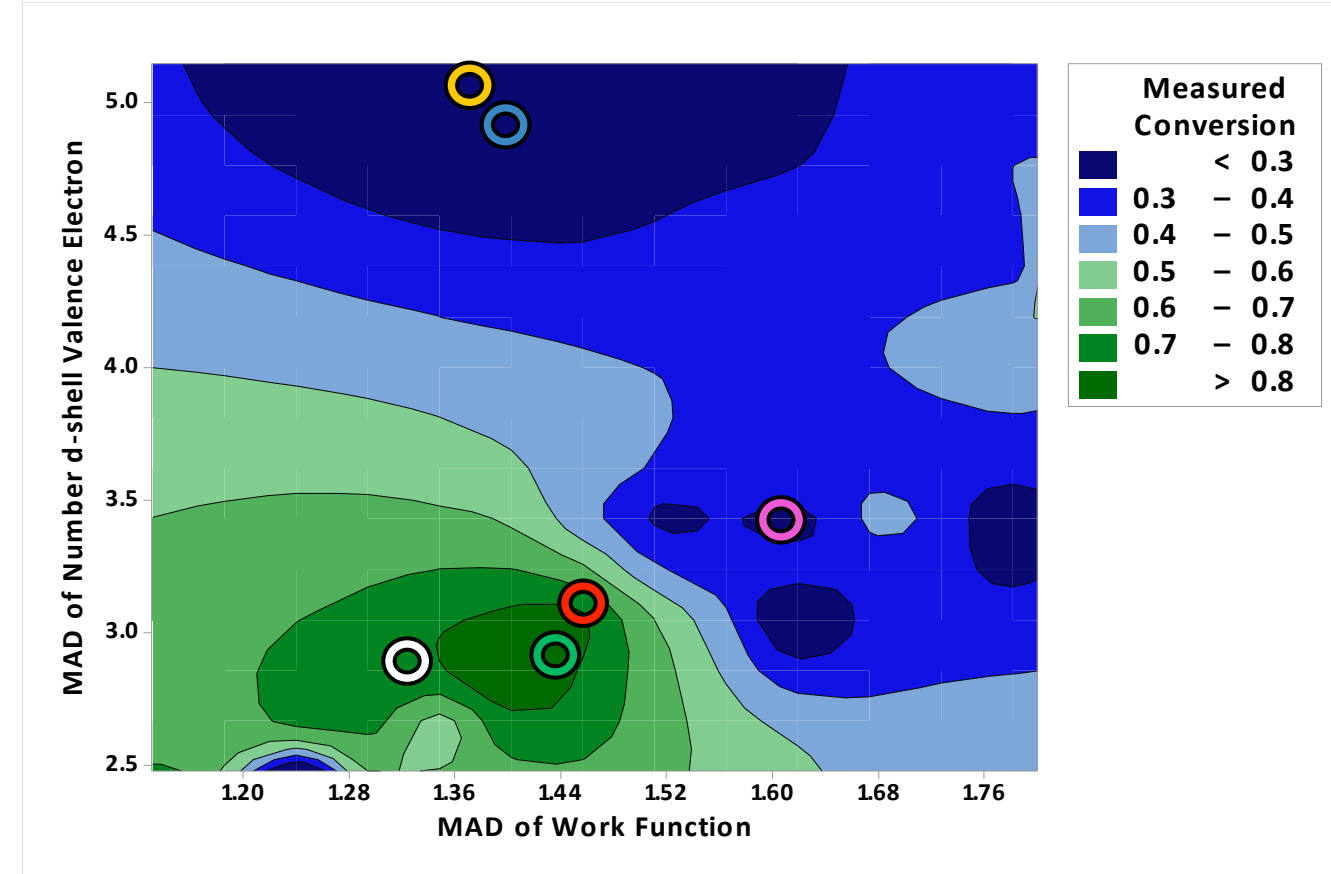
(○) 3112 RuMgK

(○) 3112 RuHfK

(○) 2212 RuInK

(○) 1312 RuZnK

(○) 3112 RuMoK

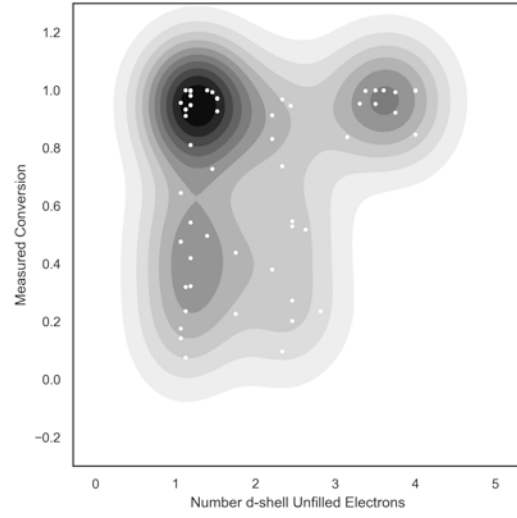
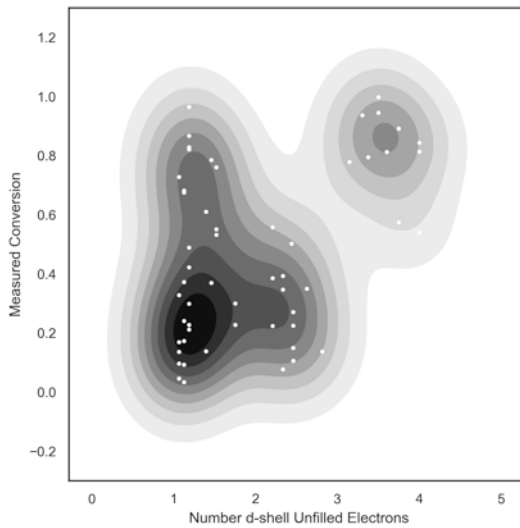
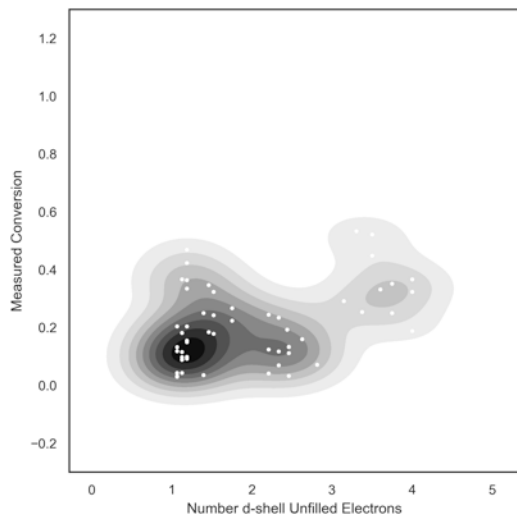


Vayenas et al., Nature 1990. 343, 625-627.

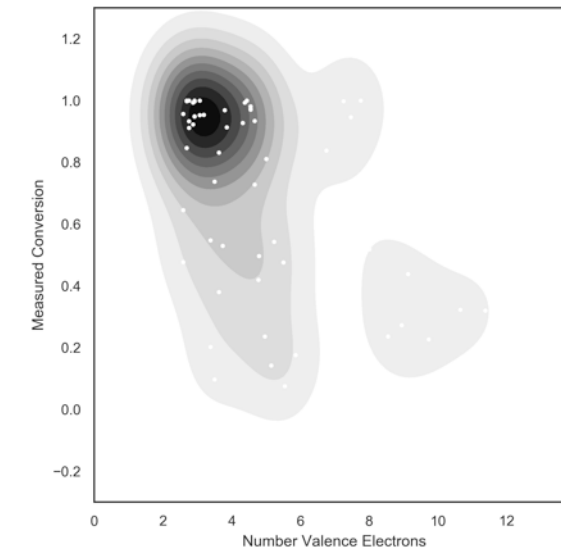
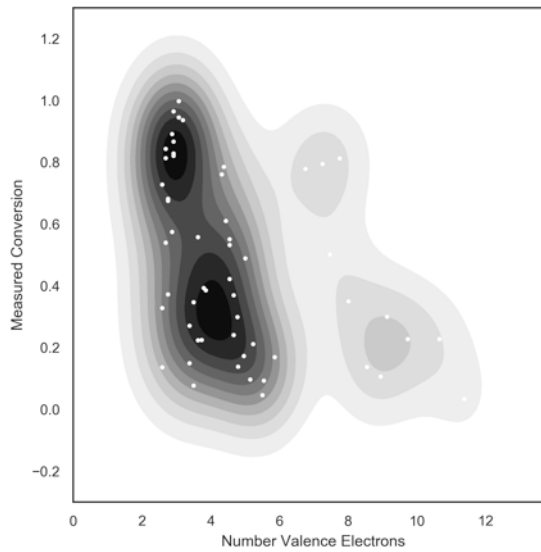
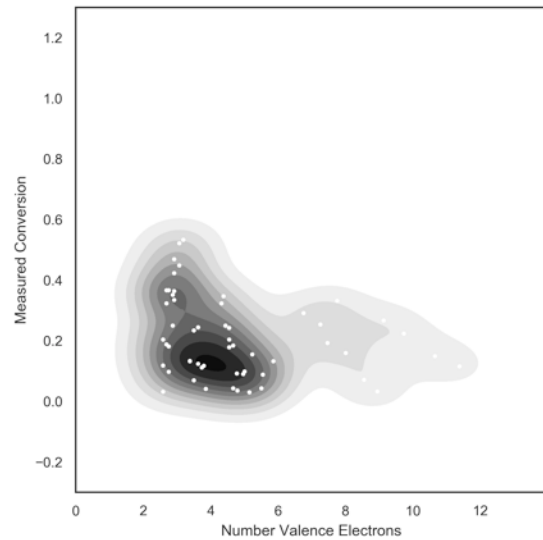
Haller, J. Catal. 216 (2003) 12-22.

Binninger et al., Phys. Rev. B. 96, 165405 (2017).

250 300 350_mad
dshell unfilled

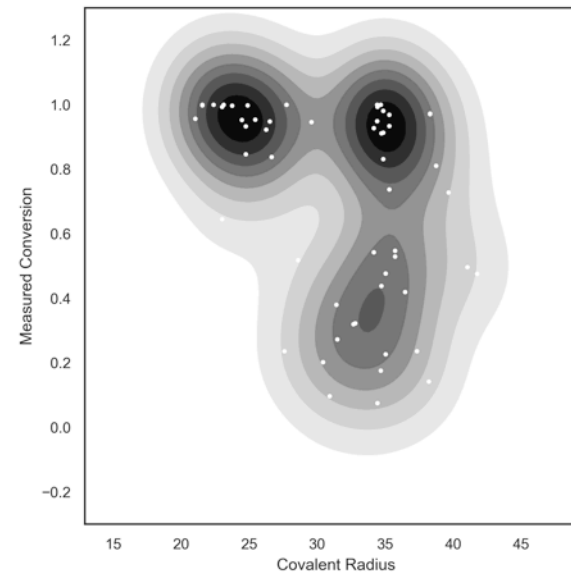
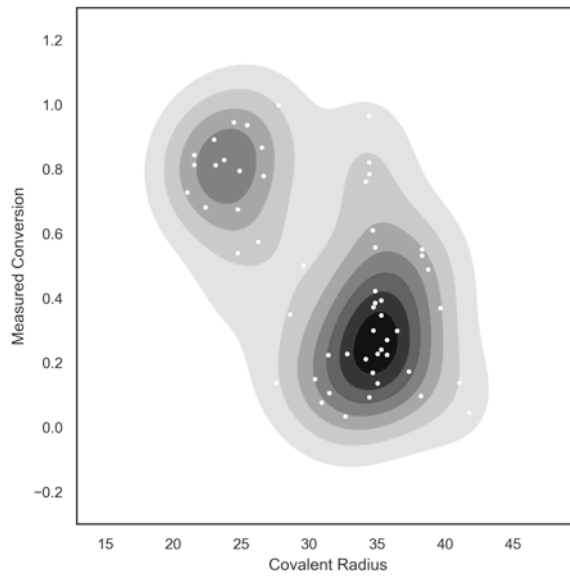
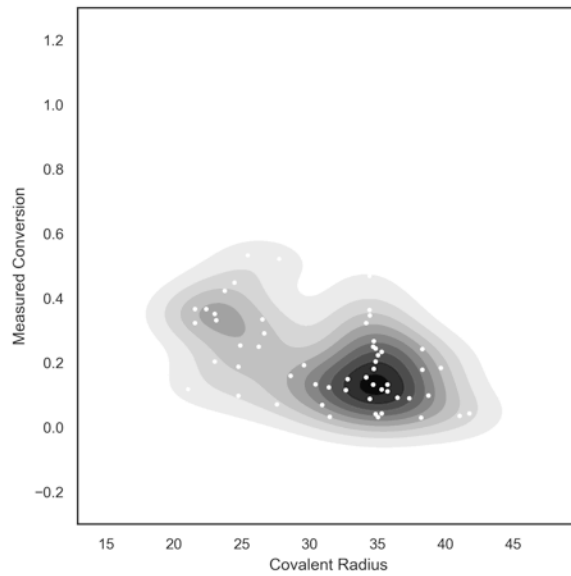


250 300 350_mad
valence



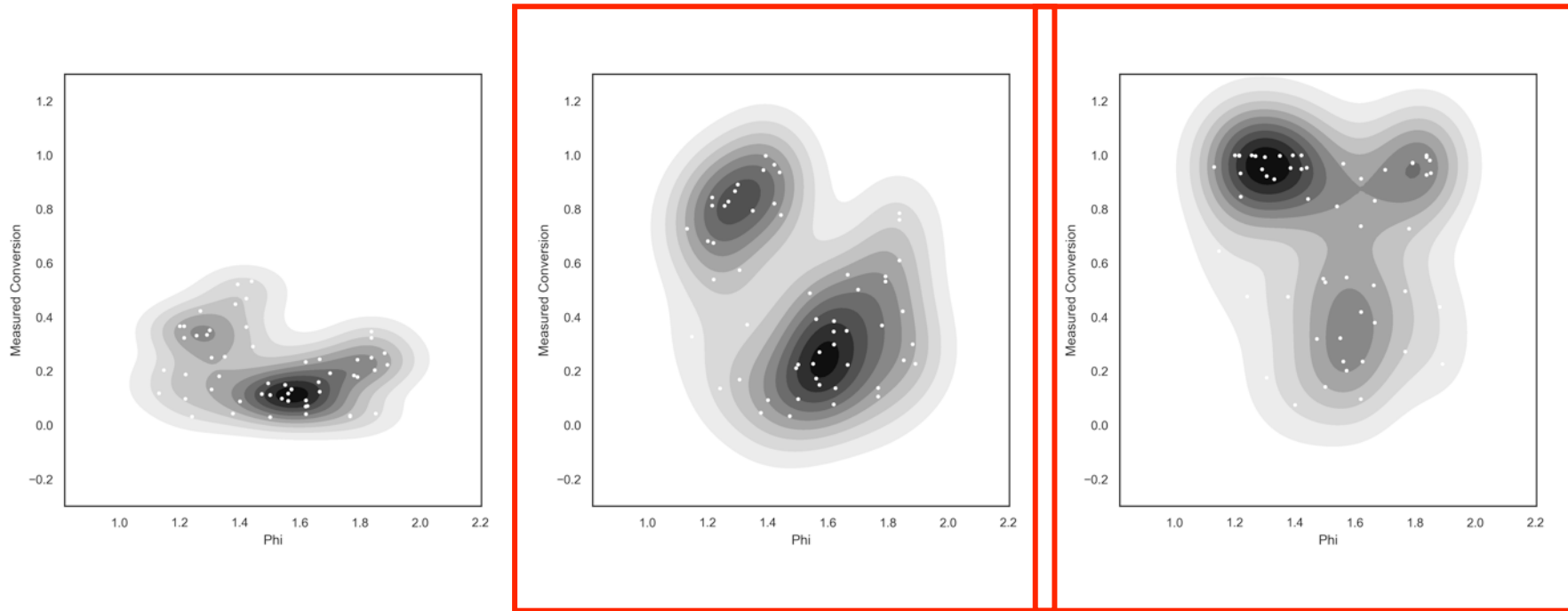
250 300 350 _mad

Covalent radius

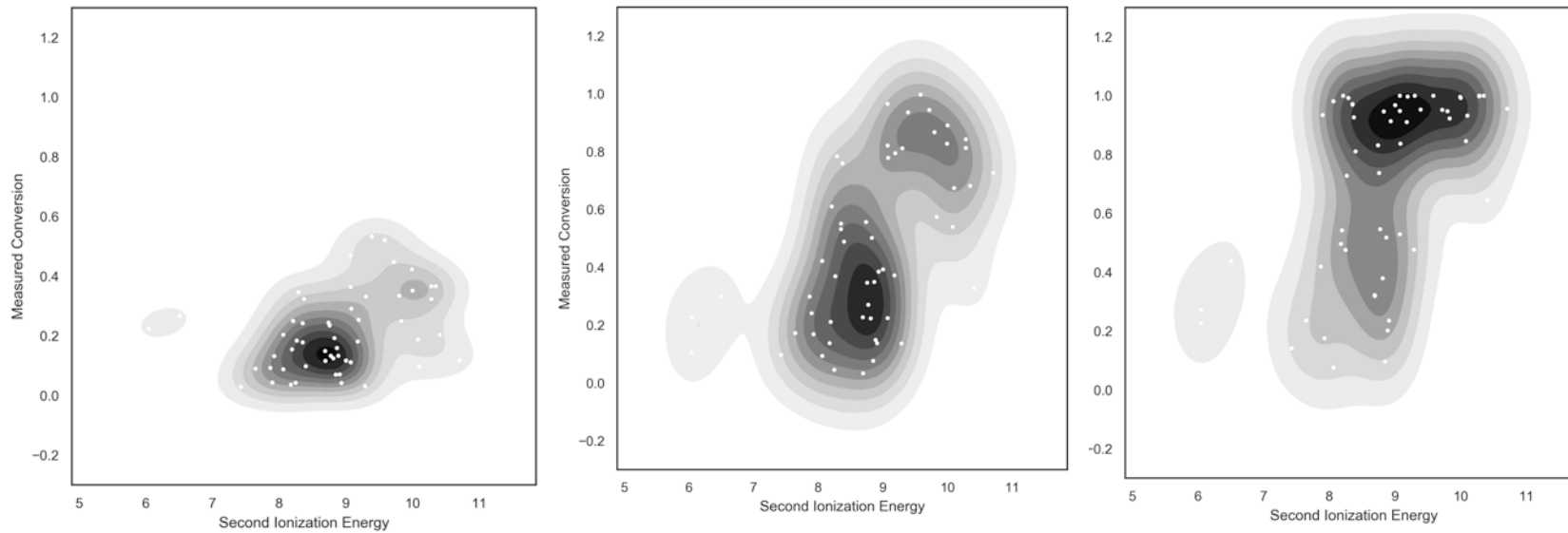


250 300 350_mad

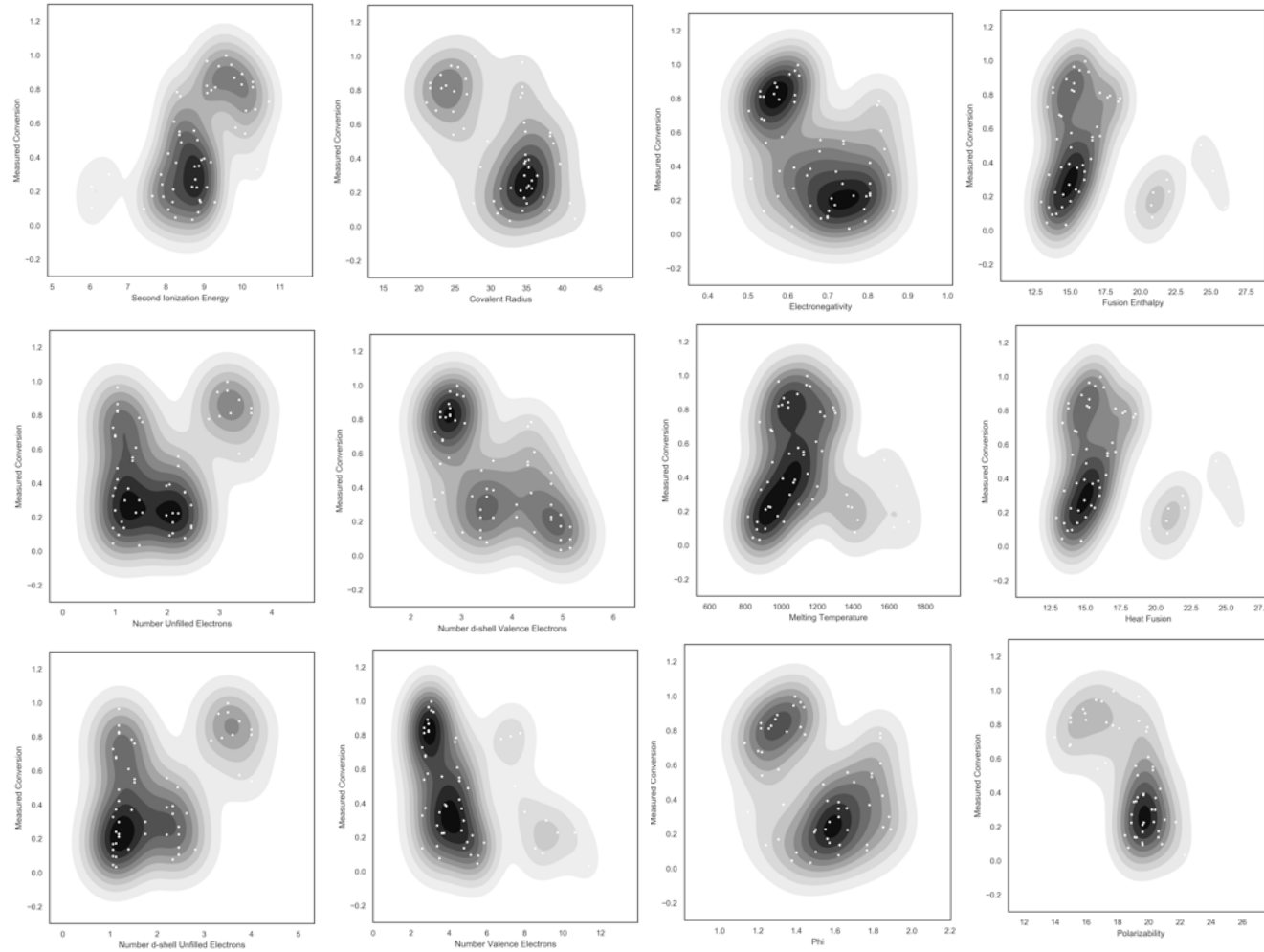
Work Function



250 300 350_mad 2nd ionization E



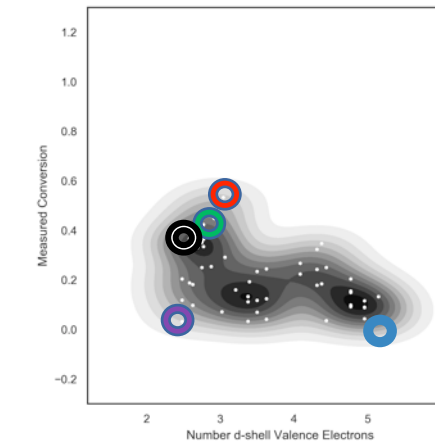
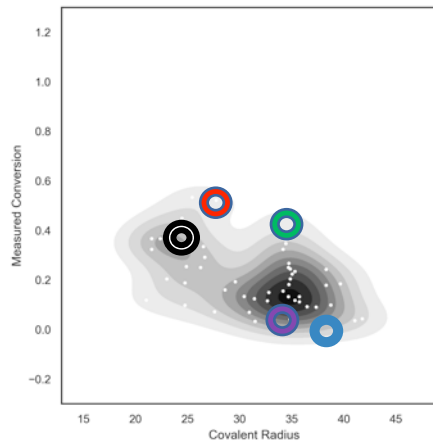
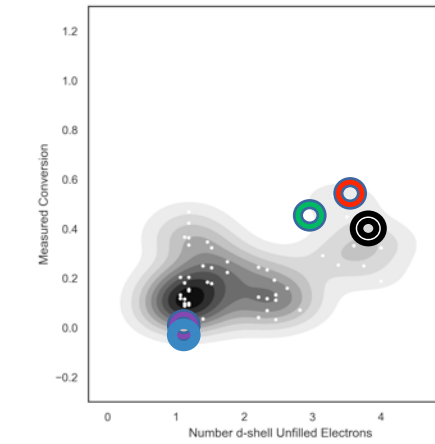
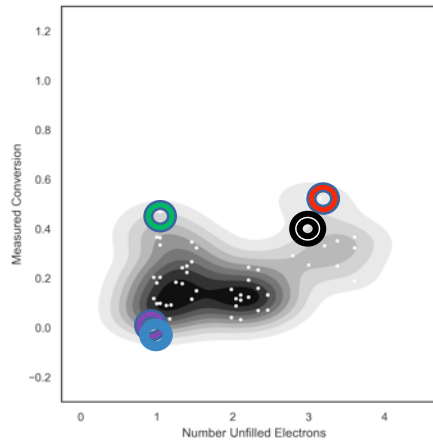
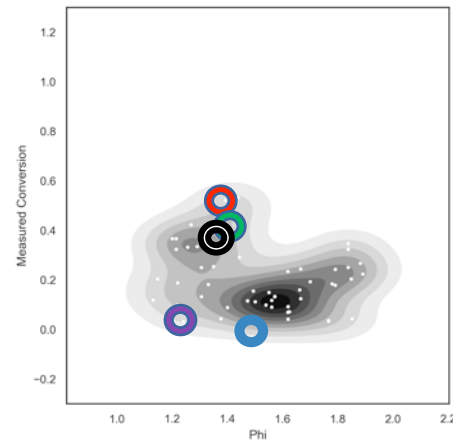
300 mad



250

top_mad

- 3112 RuYK
- 3112 RuScK
- 3112 RuMgK
- 1312 RuMgK
- 1312 RuCuK



350 top_mad

